Chem Soc Rev

This article was published as part of the

2009 Renewable Energy issue

Reviewing the latest developments in renewable energy research

Guest Editors Professor Daniel Nocera and Professor Dirk Guldi

Please take a look at the issue 1 table of contents to access the other reviews.

Heterogeneous photocatalyst materials for water splitting†

Akihiko Kudo* and Yugo Miseki

Received 8th October 2008
First published as an Advance Article on the web 18th November 2008
DOI: 10.1039/b800489g

This *critical review* shows the basis of photocatalytic water splitting and experimental points, and surveys heterogeneous photocatalyst materials for water splitting into H_2 and O_2, and H_2 or O_2 evolution from an aqueous solution containing a sacrificial reagent. Many oxides consisting of metal cations with d^0 and d^{10} configurations, metal (oxy)sulfide and metal (oxy)nitride photocatalysts have been reported, especially during the latest decade. The fruitful photocatalyst library gives important information on factors affecting photocatalytic performances and design of new materials. Photocatalytic water splitting and H_2 evolution using abundant compounds as electron donors are expected to contribute to construction of a clean and simple system for solar hydrogen production, and a solution of global energy and environmental issues in the future (361 references).

1. Introduction

Energy and environmental issues at a global level are important topics. It is indispensable to construct clean energy systems in order to solve the issues. Hydrogen will play an important role in the system because it is an ultimate clean energy and it can be used in fuel cells. Moreover, hydrogen is used in chemical industries. For example, a large amount of hydrogen is consumed in industrial ammonia synthesis. At present, hydrogen is mainly produced from fossil fuels such as natural gas by steam reforming.

$$CH_4 + H_2O \rightarrow CO + 3H_2 \quad (1)$$

$$CO + H_2O \rightarrow CO_2 + H_2 \quad (2)$$

Faculty of Science, Tokyo University of Science, 1-3 Kagurazaka, Shinjuku-ku, Tokyo 162-1861, Japan.
E-mail: a-kudo@rs.kagu.tus.ac.jp; Fax: +81-35261-4631; Tel: +81-35228-8267

† Part of the renewable energy theme issue.

In this process, fossil fuels are consumed and CO_2 is emitted. Hydrogen has to be produced from water using natural energies such as sunlight if one thinks of energy and environmental issues. Therefore, achievement of solar hydrogen production from water has been urged. There are several ways for solar hydrogen production.

(i) Electrolysis of water using a solar cell, a hydroelectric power generation, *etc*.

(ii) Reforming of biomass.

(iii) Photocatalytic or photoelectrochemical water splitting (artificial photosynthesis).

The characteristic point of water splitting using a powdered photocatalyst is the simplicity as shown in Fig. 1. Sun shines at photocatalyst powders dispersed in a pool with water, and then hydrogen is readily obtained. The necessity of separation of H_2 evolved from O_2 is disadvantageous toward the photocatalytic water splitting process. However, the problem will be able to be overcome using a *Z*-scheme photocatalyst system.

Akihiko Kudo

Akihiko Kudo was born in Tokyo. He received his early education at Tokyo University of Science obtaining a BS degree in 1983 and his PhD degree in 1988 from Tokyo Institute of Technology. After one and half years as a post-doctoral fellow at the University of Texas at Austin he became a Research Associate at the Tokyo Institute of Technology until 1995. He then joined the Tokyo University of Science as a Lecturer before he became Associate Professor in 1998 and Full Professor in 2003. His research interests include photocatalysts for water splitting, electrocatalysis and luminescence materials.

Yugo Miseki

Yugo Miseki was born in Tokyo. He received BS and MS degrees from Tokyo University of Science in 2004 and 2006, respectively. He is currently on a doctorate course in Tokyo University of Science under the supervision of Professor Akihiko Kudo. His research interests include the development of novel photocatalysts for water splitting.

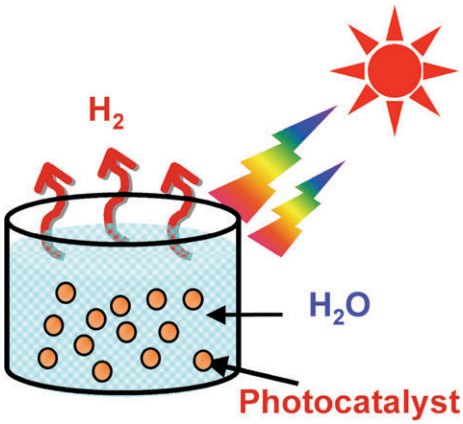

Fig. 1 Solar hydrogen production from water using a powdered photocatalyst.

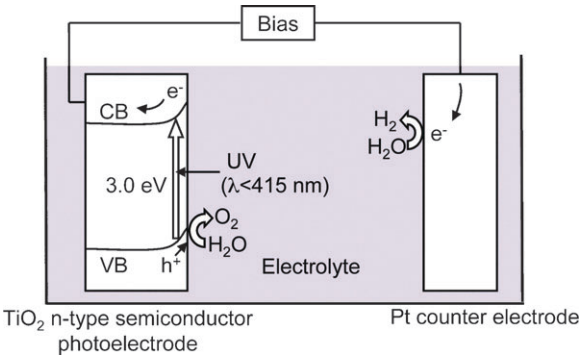

Fig. 3 Honda–Fujishima effect-water splitting using a TiO_2 photoelectrode.[3]

Moreover, powdered photocatalyst systems will be advantageous for large-scale application of solar water splitting because of the simplicity. So, photocatalytic water splitting is an attractive reaction and will contribute to an ultimate green sustainable chemistry and solving energy and environmental issues resulting in bringing an energy revolution.

The photon energy is converted to chemical energy accompanied with a largely positive change in the Gibbs free energy through water splitting as shown in Fig. 2. This reaction is similar to photosynthesis by green plants because these are uphill reactions. Therefore, photocatalytic water splitting is regarded as an artificial photosynthesis and is an attractive and challenging theme in chemistry. From the viewpoint of the Gibbs free energy change, photocatalytic water splitting is distinguished from photocatalytic degradation reactions such as photo-oxidation of organic compounds using oxygen molecules that are generally downhill reactions. This downhill-type reaction is regarded as a photoinduced reaction and has been extensively studied using TiO_2 photocatalysts.[1,2]

The Honda–Fujishima effect of water splitting using a TiO_2 electrode was reported in the early 1970s. When TiO_2 is irradiated with UV light electrons and holes are generated as shown in Fig. 3.[3] The photogenerated electrons reduce water to form H_2 on a Pt counter electrode while holes oxidize water to form O_2 on the TiO_2 electrode with some external bias by a power supply or pH difference between a catholyte and an anolyte. Numerous researchers had extensively studied water splitting using semiconductor photoelectrodes and photocatalysts since the finding. However, efficient materials for water splitting into H_2 and O_2 under visible light irradiation had not been found. Accordingly, the photon energy conversion by water splitting using photocatalysts had been considered to be pessimistic, and its research activity had been sluggish. However, new photocatalyst materials for water splitting have recently been discovered one after another. Although the photon energy conversion using powdered photocatalysts is not at the stage of practical use, the research in photocatalytic water splitting is being advanced. The photocatalytic water splitting is still a challenging reaction even if the research history is long.

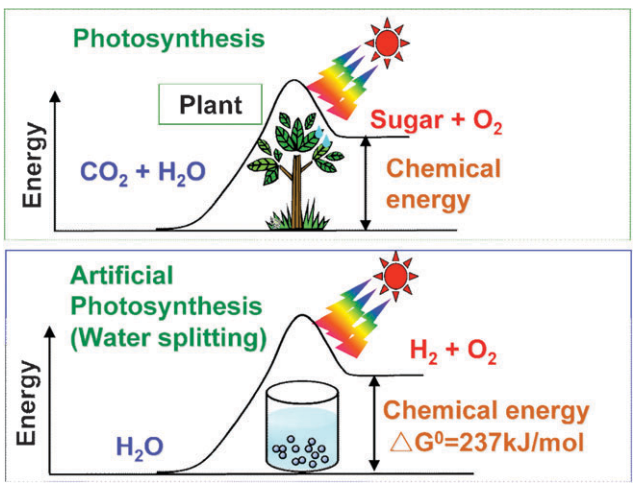

Fig. 2 Photosynthesis by green plants and photocatalytic water splitting as an artificial photosynthesis.

Many reviews and books for photocatalytic water splitting have been published.[4–30] In the present review, we focus on heterogeneous photocatalyst materials of metal oxides, metal (oxy)sulfides and metal (oxy)nitrides for water splitting into H_2 and O_2 in stoichiometric amount, and H_2 or O_2 evolution from an aqueous solution containing a sacrificial reagent. After the bases of photocatalytic water splitting are interpreted heterogeneous photocatalyst materials are surveyed. Factors affecting photocatalytic performances and strategies of photocatalyst design are discussed through the general viewpoint. Some applications of newly developed photocatalysts to other photocatalytic reactions such as degradation of organic compounds are also introduced.

2. Bases of photocatalytic water splitting

2.1 Processes in photocatalytic water splitting

Fig. 4 shows the main processes in a photocatalytic reaction.

The first step (i) is absorption of photons to form electron–hole pairs. Many heterogeneous photocatalysts have semiconductor properties. Photocatalytic reactions proceed on semiconductor materials as schematically shown in Fig. 5. Semiconductors have a band structure in which the conduction band is separated from the valence band by a band gap

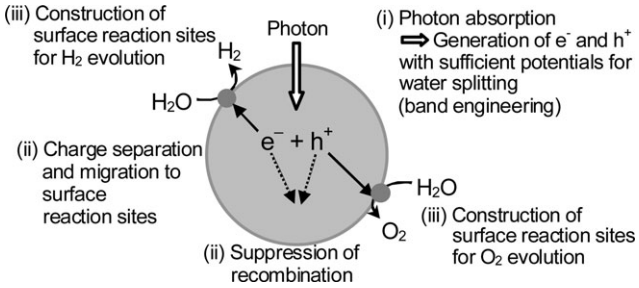

Fig. 4 Main processes in photocatalytic water splitting.

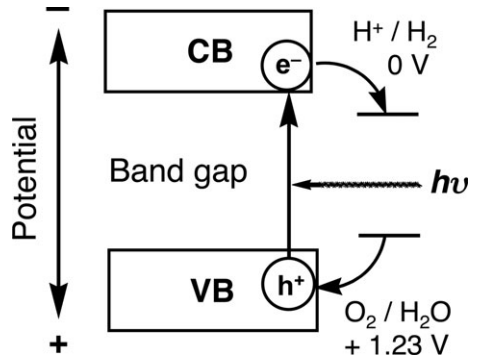

Fig. 5 Principle of water splitting using semiconductor photocatalysts.

with a suitable width. When the energy of incident light is larger than that of a band gap, electrons and holes are generated in the conduction and valence bands, respectively. The photogenerated electrons and holes cause redox reactions similarly to electrolysis. Water molecules are reduced by the electrons to form H_2 and are oxidized by the holes to form O_2 for overall water splitting. Important points in the semiconductor photocatalyst materials are the width of the band gap and levels of the conduction and valence bands. The bottom level of the conduction band has to be more negative than the redox potential of H^+/H_2 (0 V *vs.* NHE), while the top level of the valence band be more positive than the redox potential of O_2/H_2O (1.23 V). Therefore, the theoretical minimum band gap for water splitting is 1.23 eV that corresponds to light of about 1100 nm.

$$\text{Band gap (eV)} = 1240/\lambda\ \text{(nm)} \qquad (3)$$

Band levels of various semiconductor materials are shown in Fig. 6. The band levels usually shift with a change in pH (−0.059 V/pH) for oxide materials.[4,29,30] ZrO_2, $KTaO_3$, $SrTiO_3$ and TiO_2 possess suitable band structures for water splitting. These materials are active for water splitting when they are suitably modified with co-catalysts. Although CdS seems to have a suitable band position and a band gap with visible light response it is not active for water splitting into H_2 and O_2. S^{2-} in CdS rather than H_2O is oxidized by photogenerated holes accompanied with elution of Cd^{2+} according to the eqn (4).[30]

$$CdS + 2h^+ \rightarrow Cd^{2+} + S \qquad (4)$$

This reaction is called photocorrosion and is often a demerit of a metal sulfide photocatalyst. ZnO is also photo-

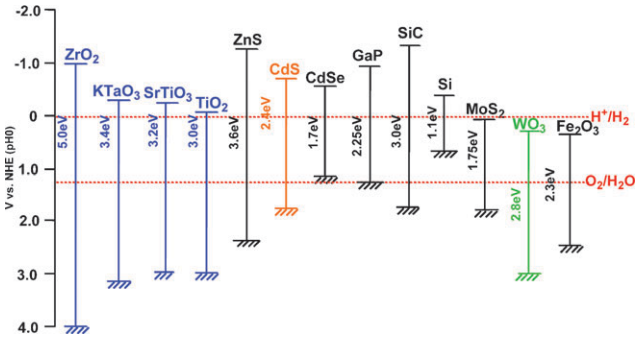

Fig. 6 Relationship between band structure of semiconductor and redox potentials of water splitting.[5]

corroded under band gap excitation even if it is an oxide photocatalyst.

$$ZnO + 2h^+ \rightarrow Zn^{2+} + 1/2O_2 \qquad (5)$$

However, CdS is an excellent photocatalyst for H_2 evolution under visible light irradiation if a hole scavenger exists as mentioned in section 2.2. On the other hand, WO_3 is a good photocatalyst for O_2 evolution under visible light irradiation in the presence of an electron acceptor such as Ag^+ and Fe^{3+} but is not active for H_2 evolution because of its low conduction band level. The band structure is just a thermodynamic requirement but not a sufficient condition. The band gap of a visible-light-driven photocatalyst should be narrower than 3.0 eV ($\lambda > 415$ nm). Therefore, suitable band engineering is necessary for the design of photocatalysts with visible light response as mentioned in section 7.1.1.

The second step (ii) in Fig. 4 consists of charge separation and migration of photogenerated carriers. Crystal structure, crystallinity and particle size strongly affect the step as shown in Fig. 7. The higher the crystalline quality is, the smaller the amount of defects is. The defects operate as trapping and recombination centers between photogenerated electrons and holes, resulting in a decrease in the photocatalytic activity. If the particle size becomes small, the distance that photogenerated electrons and holes have to migrate to reaction sites on the surface becomes short and this results in a decrease in the recombination probability.

The final step (iii) in Fig. 4 involves the surface chemical reactions. The important points for this step are surface character (active sites) and quantity (surface area). Even if the photogenerated electrons and holes possess

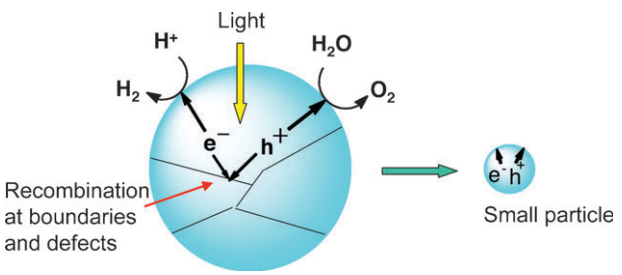

Fig. 7 Effects of particle size and boundary on photocatalytic activity.

thermodynamically sufficient potentials for water splitting, they will have to recombine with each other if the active sites for redox reactions do not exist on the surface. Co-catalysts such as Pt, NiO and RuO_2 are usually loaded to introduce active sites for H_2 evolution because the conduction band levels of many oxide photocatalysts are not high enough to reduce water to produce H_2 without catalytic assistance. Active sites for 4-electron oxidation of water are required for O_2 evolution. Co-catalysts are usually unnecessary for oxide photocatalysts because the valence band is deep enough to oxidize water to form O_2 as mentioned in section 7.1.1. This is the characteristic point of heterogeneous photocatalysts being different from homogeneous photocatalysts for which O_2 evolution with 4-electron oxidation of H_2O is a challenging reaction. Back reactions to form water by reactions between evolved H_2, O_2, and intermediates easily proceed because of an uphill reaction. Therefore, poor properties for the back reactions are required for the surface of co-catalyst and photocatalyst.

Fig. 8 shows how the processes indicated in Fig. 4 are affected by conditions of a photocatalyst in the case of TiO_2. The TiO_2 photocatalyst is prepared by several methods. For example, amorphous TiO_2 that may be denoted as $TiO_2{\cdot}nH_2O$ is obtained by hydrolysis of titanium tetra-isopropoxide. When the amorphous TiO_2 is calcined some factors are simultaneously changed. Anatase and rutile are obtained through phase transition. The band gap of anatase is 3.2 eV while that of rutile is 3.0 eV indicating that the crystal structure determines the band gap even if the composition is the same. The difference in the band gap between anatase and rutile is mainly due to the difference in the conduction band level. The conduction band level of anatase is higher than that of rutile leading the difference in photocatalytic abilities between anatase and rutile (brookite TiO_2 is selectively prepared by a hydrothermal method).[31] Crystallinity is increased by calcination: that is a positive factor as shown in Fig. 7. The crystallinity is confirmed from half-widths of peaks of XRD patterns and also observation by electron microscopes. On the other hand, the surface area (as determined by BET measurement) is decreased with an increase in particle size through sintering: that is a negative factor. Small particle size sometimes gives a quantum size effect as seen in colloidal particles resulting in widening of band gap and blue shift in the absorption spectrum. The resultant photocatalytic activity is dominated by the balance among these factors. A high degree of crystallinity is often required rather than a high surface area for water splitting because recombination between photogenerated electrons and holes is especially a serious problem for uphill reactions. In contrast, high surface area is necessary for photocatalytic degradation of organic compounds because adsorption of the organic compound is the important process. Concentration of surface hydroxyl groups may also affect photocatalytic activity.[32]

Many photocatalysts are also materials for solar cells, phosphors and dielectrics. However, the significant difference between the photocatalyst and the other materials is that chemical reactions are involved in the photocatalytic process, but not in the other physical properties. Only when three steps shown in Fig. 4 are simultaneously completed photocatalytic activities can be obtained. Thus, suitable bulk and surface properties, and energy structure are required for photocatalysts. So, it is understandable that photocatalysts should be highly functional materials.

2.2 Photocatalytic H_2 or O_2 evolution in sacrificial systems

Sacrificial reagents are often employed to evaluate the photocatalytic activity for water splitting as shown in Fig. 9, because overall water splitting is a tough reaction. When the photocatalytic reaction is carried out in an aqueous solution including a reducing reagent, in other words, electron donors or hole scavengers, such as alcohol and a sulfide ion, photogenerated holes irreversibly oxidize the reducing reagent instead of water. It enriches electrons in a photocatalyst and an H_2 evolution reaction is enhanced as shown in Fig. 9(a). This reaction will be meaningful for realistic hydrogen production if biomass and abundant compounds in nature and industries are used as the reducing reagents.[33–38] On the other hand, photogenerated electrons in the conduction band are consumed by oxidizing reagents (electron acceptors or electron scavengers) such as Ag^+ and Fe^{3+} resulting in that an O_2 evolution reaction is enhanced as shown in Fig. 9(b). These reactions using sacrificial reagents are studied to evaluate if a certain photocatalyst satisfies the thermodynamic and kinetic potentials for H_2 and O_2 evolution. These reactions are regarded as half reactions of water splitting and are often employed as test reactions of photocatalytic H_2 or O_2 evolution as mentioned in sections 6 and 7.

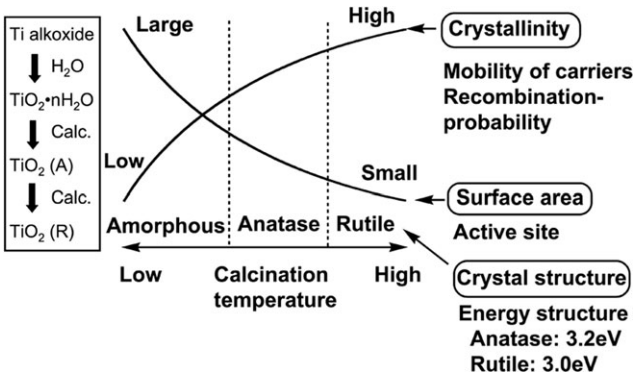

Fig. 8 Conditions affecting photocatalytic activity of TiO_2.

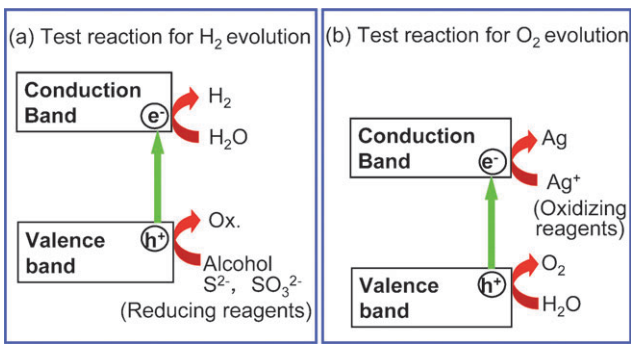

Fig. 9 H_2 or O_2 evolution reaction in the presence of sacrificial reagents—Half reactions of water splitting.

Even if a photocatalyst is active for these half reactions the results do not guarantee a photocatalyst to be active for overall water splitting into H_2 and O_2 in the absence of sacrificial reagents. From this point, the term of "water splitting" should be distinguishably used for H_2 or O_2 evolution from aqueous solutions in the presence of sacrificial reagents. Water splitting means to split water into H_2 and O_2 in a stoichiometric amount in the absence of sacrificial reagents.

3. Experimental method for water splitting

3.1 Points that should be paid attention

The points that should be paid attention to evaluate photocatalytic water splitting are shown in Fig. 10.[7]

(i) Stoichiometry of H_2 and O_2 evolution. In water splitting, both H_2 and O_2 should form with a stoichiometric amount, 2:1, in the absence of a sacrificial reagent. Often H_2 evolution is observed with a lack of O_2 evolution. In this case, the amount of H_2 evolution is usually small compared with an amount of a photocatalyst. It is not clear if such a reaction is photocatalytic water splitting and it is important to clarify that it is not a sacrificial reaction.

(ii) Time course. Amounts of H_2 and O_2 evolved should increase with irradiation time. To check not only the value of activity or a gas evolution rate but also the time course is important. Repeated experiment is also informative.

(iii) Turnover number (TON). Amounts of H_2 and O_2 should overwhelm an amount of a photocatalyst. If the amounts are much less than the amount of photocatalyst we do not know if the reaction proceeds photocatalytically because the reaction might be due to some stoichiometric reactions. Turnover number (TON) is usually defined by the number of reacted molecules to that of an active site (eqn (6)).

$$\mathrm{TON} = \frac{\text{Number of reacted molecules}}{\text{Number of active sites}} \qquad (6)$$

However, it is often difficult to determine the number of active sites for photocatalysts. Therefore, the number of reacted electrons to the number of atoms in a photocatalyst (eqn (7)) or on the surface of a photocatalyst (eqn (8)) is employed as the TON.

$$\mathrm{TON} = \frac{\text{Number of reacted electrons}}{\text{Number of atoms in a photocatalyst}} \qquad (7)$$

$$\mathrm{TON} = \frac{\text{Number of reacted electrons}}{\text{Number of atoms at the surface of a photocatalyst}} \qquad (8)$$

The number of reacted electrons is calculated from the amount of evolved H_2. The TONs (7) and (8) are smaller than the real TON (6) because the number of atoms is more than that of active sites. Normalization of photocatalytic activity by weight of used photocatalyst (for example, μmol h^{-1} g^{-1}) is not acceptable because the photocatalytic activity is not usually proportional to the weight of photocatalyst if an amount of photocatalyst is enough for a certain experimental condition. The amount of photocatalyst should be optimized for an each experimental setup. In this case, photocatalytic activity usually depends on the number of photons absorbed by a photocatalyst unless the light intensity is too strong.

(iv) Quantum yield. The rate of gas evolution is usually indicated with a unit, for example μmol h^{-1}. Because the photocatalytic activity depends on the experimental conditions such as a light source and a type of a reaction cell, the activities cannot be compared with each other if the reaction conditions are different from each other. Therefore, determination of a quantum yield is important. The number of incident photons can be measured using a thermopile or Si photodiode. However, it is hard to determine the real amount of photons absorbed by a photocatalyst in a dispersed system because of scattering. So, the obtained quantum yield is an apparent quantum yield (9). The apparent quantum yield is estimated to be smaller than the real quantum yield because the number of absorbed photons is usually smaller than that of incident light.

$$\mathrm{AQY}\ (\%) = \frac{\text{Number of reacted electrons}}{\text{Bumber of incident photons}} \times 100 \qquad (9)$$

It should be noteworthy that the quantum yield is different from the solar energy conversion efficiency that is usually used for evaluation of solar cells.

$$\text{Solar energy conversion}\ (\%) = \frac{\text{Output energy as } H_2}{\text{Energy of incident solar light}} \times 100 \qquad (10)$$

The number of photocatalysts that can give good solar energy conversion efficiency is limited at the present stage because of insufficient activities for the measurement. However, the solar energy conversion efficiency should finally be used to evaluate the photocatalytic water splitting if solar hydrogen production is considered.

(v) Photoresponse. When a photocatalyst is irradiated with light of energy larger than the band gap, water splitting should proceed. An action spectrum is indispensable to see the photoresponse, especially for a photocatalyst with visible light response (band-path and interference filters are usually

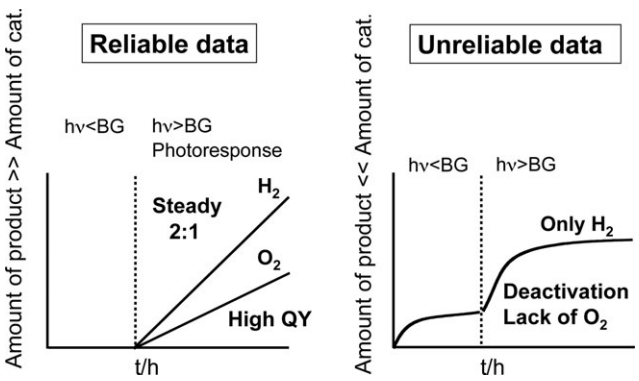

Fig. 10 Important points for evaluation of data for photocatalytic water splitting.

employed to obtain monochromatic light for the action spectrum measurement). Even if a material absorbs visible light it does not always show a photocatalytic activity by the excitation of the visible light absorption band. Cut-off filters are sometimes used to see the photoresponse. In this case the onset of the photoresponse can be measured. Water splitting by mechanocatalysis proceeds on some metal oxides under stirring and dark condition.[8,39] Some control experiments such as no photocatalysts or non-irradiation have to be carried out to confirm the photocatalytic reaction and neglect the possibility of the mechanocatalytic water splitting.

There are many other points that researchers have to pay attention. The details of experiments for general photocatalysis are described in the literature by Ohtani.[40]

3.2 Experimental setup

There are several types of apparatus for water splitting. The present authors have usually used a gas-closed circulation system equipped with a vacuum line, a reaction cell and a gas sampling port that is directly connected to a gas chromatograph as shown in Fig. 11. If a photocatalytic activity is too high to use a gas chromatograph a volumetric method is employed for determination of evolved gases. The apparatus should be air-free because the detection of O_2 is very important for evaluation of photocatalytic water splitting. There are several reaction cells. In general, efficient irradiation is conducted when an inner irradiation reaction cell is used. A high-pressure mercury lamp is often used with a quartz cell for photocatalysts with wide band gaps when intensive UV light with wavelength shorter than about 300 nm is especially needed. When visible light irradiation is necessary a Xe-lamp with a cut-off filter is usually employed. It is important to know the spectrum of the incident light. It depends on a light source, a material of a reaction cell, an optical filter, a mirror, *etc*. A solar simulator that is a standard light source for evaluation of solar cells should ideally be used if solar hydrogen production is considered. A solar simulator with an air-mass 1.5 filter (AM-1.5) irradiates 100 mW cm^{-2} of power.

4. General view of elements constructing heterogeneous photocatalyst materials

Fig. 12 shows elements constructing heterogeneous photocatalyst materials. The elements are classified into four groups; (i) to construct crystal structure and energy structure, (ii) to construct crystal structure but not energy structure, (iii) to form impurity levels as dopants and (iv) to be used as co-catalysts.

Most metal oxide, sulfide and nitride photocatalysts consist of metal cations with d^0 and d^{10} configurations. Their conduction bands for the d^0 and d^{10} metal oxide photocatalysts are usually composed of d and sp orbitals, respectively, while their valence bands consist of O 2p orbitals. Valence bands of metal sulfide and nitride photocatalysts are usually composed of S 3p and N 2p orbitals, respectively. Orbitals of Cu 3d in Cu^+, Ag 4d in Ag^+, Pb 6s in Pb^{2+}, Bi 6s in Bi^{3+}, and Sn 5s in Sn^{2+} can also form valence bands in some metal oxide and sulfide photocatalysts as mentioned in sections 7.1.4 and 9.3.

Alkali, alkaline earth and some lanthanide ions do not directly contribute to the band formation and simply construct the crystal structure as A site cations in perovskite compounds.

Some transition metal cations with partially filled d orbitals such as Cr^{3+}, Ni^{2+} and Rh^{3+} form some impurity levels in band gaps when they are doped or substituted for native metal cations. Although they often work as recombination centres between photogenerated electrons and holes they sometimes play an important role for visible light response as mentioned in sections 7.1.3 and 9.2.

Some transition metals and the oxides such as noble metals (Pt,[41,42] Rh[42,43] and Au[44,45]), NiO[46] and RuO_2[47,48] function as co-catalysts for H_2 evolution. In water splitting, a back reaction to form water from evolved H_2 and O_2 has to be suppressed because of an uphill reaction. Au, NiO and RuO_2 are suitable co-catalysts on which the back reaction hardly proceeds. A Cr–Rh oxide has recently been found as an excellent co-catalyst for H_2 evolution by oxynitride photocatalysts.[49,50] IrO_2 colloids works as an O_2 evolution co-catalyst.[51–53]

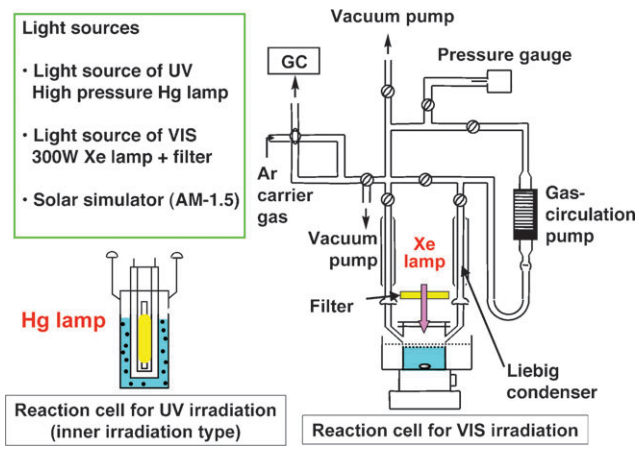

Fig. 11 An example of the experimental setup for photocatalytic water splitting.

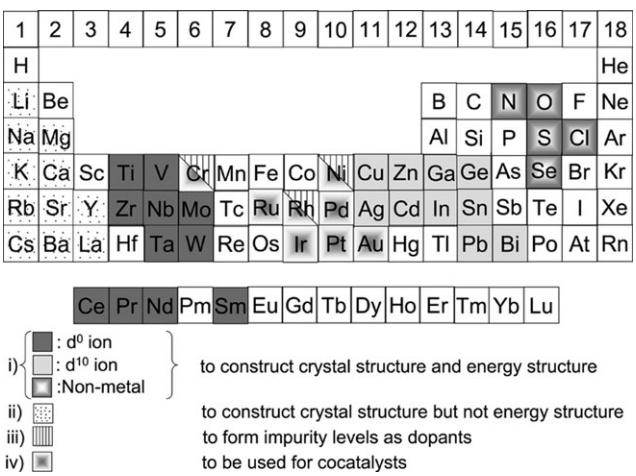

Fig. 12 Elements constructing heterogeneous photocatalysts.

5. Wide band gap metal oxide photocatalysts for water splitting under UV irradiation

5.1 Oxide photocatalysts consisting of d^0 metal cations[42–43,45,46,54–151]

Table 1 shows photocatalyst materials consisting of d^0 metal cations (Ti^{4+}, Zr^{4+}, Nb^{5+}, Ta^{5+} and W^{6+}) for water splitting with reasonable activities. The activities are not directly compared with each other because experimental conditions such as light sources, reaction cells, and the scale of the reaction are different from each other. But the values of activities would make sense as to how high the activities of photocatalysts are.

Valence bands of these photocatalysts, except for $AgTaO_3$, consist of O 2p orbitals of which the potential is about 3 eV *vs.* NHE while conduction band levels are more negative than 0 eV. It results in that these materials respond to only UV. An Ag 4d orbital forms a valence band of $AgTaO_3$ with a O 2p orbital.[125]

These metal mixed oxides are usually prepared by a solid-state reaction. Metal oxides and/or alkali and alkaline earth carbonates of starting materials are calcined at high temperature in air.

A polymerizable complex method[152] is sometimes used for preparation of photocatalysts.[68,74,80,111,112,134,143] This preparation method gives fine and well-crystalline powders with a high surface area at relatively low calcination temperature and short calcination time compared with a conventional solid state method. The example of an $Sr_2Ta_2O_7$ photocatalyst is shown in Fig. 13.[111] $SrCO_3$ and $TaCl_5$ are dissolved in an ethylene glycol (EG) and methanol mixed solution containing anhydrous citric acid (CA) of a chelating agent to stabilize metal cations. The transparent colourless solution is heated at 403 K with stirring to promote polymerization between CA and EG. The solution becomes more viscous with time, and a brown resin-like gel is obtained without any visible precipitation after several hours. The brown gel is heated at 723 K for several hours to remove residual solvents and to burn out unnecessary organics. The powder obtained is referred to as powder precursors for $Sr_2Ta_2O_7$. The powder precursor is calcined at temperatures between 973 and 1273 K for 5–100 h in air. Some metal oxide photocatalysts that are hardly prepared by solid-state reactions can be obtained by the polymerizable complex method.[143] Aqueous processes such as hydrothermal synthesis[31,131] are also employed for the preparation of photocatalysts. Photocatalysts prepared by these soft processes sometimes show higher activities than those prepared by solid state reaction because they have small particle size and good crystallinity. Next, let us see each photocatalyst.

5.1.1 Group 4 elements[42,43,46,54–97]. TiO_2 has extensively been studied for a long time. Although water splitting was firstly demonstrated using a TiO_2 photoelectrode with some external bias as shown in Fig. 3 a powdered TiO_2 photocatalyst can not split water without any modifications such as loading co-catalysts. At the initial stage of the research, it was questionable that a platinized TiO_2 photocatalyst could split water because the activity was usually low and no O_2 evolution was often observed. After that, NaOH-coating[43] and additions of alkali carbonates[55] have been found to be effective for water splitting on the Pt/TiO_2 photocatalyst.

$SrTiO_3$[29,153] and $KTaO_3$[29,154] photoelectrodes with perovskite structure can split water without an external bias being different from TiO_2 because of their high conduction band levels as shown in Fig. 6. These materials can be used as powdered photocatalysts. Domen and co-workers have reported that NiO-loaded $SrTiO_3$ powder can decompose pure water into H_2 and O_2.[46,59–63] The NiO co-catalyst for H_2 evolution is usually activated by H_2 reduction and subsequent O_2 oxidation to form a NiO/Ni double layer structure that is convenient for electron migration from a photocatalyst substrate to a co-catalyst.[61] The pretreated NiO co-catalyst is often denoted as NiO_x in literature. It is important that the NiO co-catalyst does not cause the back reaction between H_2 and O_2, being different from Pt. The excellent NiO co-catalyst has often been employed for many photocatalysts for water splitting as seen in Table 1. Rh is also a suitable co-catalyst for the $SrTiO_3$ photocatalyst.[42]

TiO_2 and $SrTiO_3$ photocatalysts are also active for reduction of NO_3^- using water as an electron donor.[155–157]

$K_2La_2Ti_3O_{10}$ that possesses a layered perovskite structure is a unique photocatalyst. H_2 evolution proceeds on a pretreated NiO_x co-catalyst while O_2 evolves at the hydrated interlayer. Many titanate, niobate and tantalate photocatalysts with layered perovskite structure have been reported since the $K_2La_2Ti_3O_{10}$ photocatalyst was found. $Sr_3Ti_2O_7$ and $Sr_4Ti_3O_{10}$ photocatalysts have perovskite slabs of $SrTiO_3$. $La_2Ti_2O_7$, $La_2Ti_2O_7$:Ba, $KLaZr_{0.3}Ti_{0.7}O_4$ and $La_4CaTi_5O_{17}$ photocatalysts with layered perovskite structure give high quantum yields.

$Na_2Ti_6O_{13}$ and $BaTi_4O_9$ with tunnel structure are also unique titanate photocatalysts. $KTiNbO_5$ shows activity when it is prepared by a polymerizable complex method. $Gd_2Ti_2O_7$ and $Y_2Ti_2O_7$ with pyrochlore structure are also active.

ZrO_2 is active without co-catalyst because of its high conduction band level. This photocatalyst is also active for CO_2 reduction to CO accompanied with O_2 evolution by oxidation of water without any sacrificial reagents.[93]

5.1.2 Group 5 elements[45,70,76,98–146]. $K_4Nb_6O_{17}$ and $Rb_4Nb_6O_{17}$ with layered structure as seen in mica show high activities. These photocatalysts possess two kinds of interlayers in which ion-exchangeable potassium cations exist as shown in Fig. 14.[100] H_2 evolution proceeds in one interlayer with a nickel co-catalyst while O_2 evolution occurs in another interlayer. It is the characteristic of the $K_4Nb_6O_{17}$ photocatalyst that H_2 evolution sites are separated from O_2 evolution sites by the photoactive niobate sheet.[101] This photocatalyst is active for water splitting and H_2 evolution from an aqueous methanol solution even without co-catalyst. Moreover, the activity for the sacrificial H_2 evolution is much enhanced by H^+-exchange.[99]

$Ca_2Nb_2O_7$, $Sr_2Nb_2O_7$ and $Ba_5Nb_4O_{15}$ with layered perovskite structure show high activity. $NaCa_2Nb_3O_{10}$ and $KCa_2Nb_3O_{10}$ stacked with RuO_2 colloids from exfoliated nano-sheets are active for water splitting although the native

Table 1 Oxide photocatalysts based on d^0 metal ions for water splitting under UV irradiation

Photocatalyst	Crystal structure	BG/eV	Co-catalyst	Light source[a]	Reactant solution	Activity/μmol h^{-1}		QY (%)	Ref. (Year)
						H_2	O_2		
Ti photocatalysts									
TiO_2	Anatase	3.2	Rh	Hg–Q	Water vapor	449		29	43 (1985)
TiO_2	Anatase	3.2	NiO_x	Hg–P	3 M NaOH	6	2		54 (1987)
TiO_2	Anatase	3.2	Pt	Hg–Q	2.2 M Na_2CO_3	568	287		55 (1997)
TiO_2	Anatase	3.2	Pt	Hg–Q	Pure water	106	53		56 (1995)
B/Ti oxide	Anatase	3.2	Pt	Hg–Q	Pure water	22	11		57 (1998)
$CaTiO_3$	Perovskite	3.5	NiO_x	Hg–Q	0.2 M NaOH	30	17		58 (2002)
$SrTiO_3$	Perovskite	3.2	NiO_x	Hg–P	5 M NaOH	40	19		46, 59–63 (1980)
$SrTiO_3$	Perovskite	3.2	Rh	Hg–Xe–P	Pure water	27	14		42, 43, 64 (1980)
$Sr_3Ti_2O_7$	Layered perovskite	3.2	NiO_x	Hg–Q	Pure water	144	72		65 (2006)
$Sr_4Ti_3O_{10}$	Layered perovskite	3.2	NiO_x	Hg–Q	Pure water	170		4.5 (at 360 nm)	66 (2002)
$K_2La_2Ti_3O_{10}$	Layered perovskite	3.4–3.5	NiO_x	Hg–Q	0.1 M KOH	2186	1131		67, 68 (1997)
$Rb_2La_2Ti_3O_{10}$	Layered perovskite	3.4–3.5	NiO_x	Hg–Q	0.1 M RbOH	869	430	5 (at 330 nm)	67 (1997)
$Cs_2La_2Ti_3O_{10}$	Layered perovskite	3.4–3.5	NiO_x	Hg–Q	Pure water	700	340		67 (1997)
$CsLa_2Ti_2NbO_{10}$	Layered perovskite	3.4–3.5	NiO_x	Hg–Q	Pure water	115	50		67 (1997)
La_2TiO_5	Layered perovskite		NiO_x	Hg–Q	Pure water	442			69 (2005)
$La_2Ti_3O_9$	Layered perovskite		NiO_x	Hg–Q	Pure water	386			69 (2005)
$La_2Ti_2O_7$	Layered perovskite	3.8	NiO_x	Hg–Q	Pure water	441		12 (<360 nm)	69–78 (1999)
$La_2Ti_2O_7$:Ba	Layered perovskite		NiO_x	Hg–Q	Pure water	5000		50	69 (2005)
$KaLaZr_{0.3}Ti_{0.7}O_4$	Layered perovskite	3.91	NiO_x	Hg–Q	Pure water	230	116	12.5	79 (2003)
$La_4CaTi_5O_{17}$	Layered perovskite	3.8	NiO_x	Hg–Q	Pure water	499		20 (<320 nm)	70 (1999)
$KTiNbO_5$	Layered structure	3.6	NiO_x	Hg–Q	Pure water	30	10		80 (1999)
$Na_2Ti_6O_{13}$	Tunnel structure		RuO_2	Xe–Q	Pure water	7.3	3.5		81–84 (1990)
$BaTi_4O_9$	Tunnel structure		RuO_2	Xe–Q	Pure water	33	16		84–90 (1992)
$Gd_2Ti_2O_7$	Cubic pyrochlore	3.5	NiO_x	Hg–Q	Pure water	400	198		76 (2006)
$Y_2Ti_2O_7$	Cubic pyrochlore	3.5	NiO_x	Hg–Q	Pure water	850	420	6 (at 313 nm)	76, 91, 92 (2004)
ZrO_2		5.0	None	Hg–Q	Pure water	72	36		93–97 (1993)
Nb photocatalysts									
$K_4Nb_6O_{17}$	Layered structure	3.4	NiO_x	Hg–Q	Pure water	1837	850	5 (at 330 nm)	45, 98–108 (1986)
$Rb_4Nb_6O_{17}$	Layered structure	3.4	NiO_x	Hg–Q	Pure water	936	451	10 (at 330 nm)	105 (1997)
$Ca_2Nb_2O_7$	Layered perovskite	4.3	NiO_x	Hg–Q	Pure water	101		7 (<288 nm)	70 (1999)
$Sr_2Nb_2O_7$	Layered perovskite	4.0	NiO_x	Hg–Q	Pure water	217	97		70, 109–111 (1999)
$Ba_5Nb_4O_{15}$	Layered perovskite	3.85	NiO_x	Hg–Q	Pure water	2366	1139	7 (at 270 nm)	112 (2006)
$NaCa_2Nb_3O_{10}$	Layered perovskite		RuO_2	Hg–Q	Pure water	118	56		113 (2005)
$ZnNb_2O_6$	Columbite	4.0	NiO_x	Hg–Q	Pure water	54	21		114 (1999)
$Cs_2Nb_4O_{11}$	Pyrochlore like	3.7	NiO_x	Hg–Q	Pure water	1700	800	3 (at 270 nm)	115 (2005)
La_3NbO_7	Cubic fluorite	3.9	NiO_x	Hg–Q	Pure water	35	17		76, 116 (2004)
Ta photocatalysts									
Ta_2O_5		4.0	NiO_x	Hg–Q	Pure water	1154	529		94, 105, 117, 118 (1994)
$K_2PrTa_5O_{15}$	Tungsten bronze	3.8	NiO	Hg–Q	Pure water	1550	830		12, 119 (2000)
$K_3Ta_3Si_2O_{13}$	Tungsten bronze	4.1	NiO	Hg–Q	Pure water	390	200		120 (1997)
$K_3Ta_3B_2O_{12}$	Tungsten bronze	4.0	None	Hg–Q	Pure water	2390	1210	6.5 (at 254 nm)	121 (2006)
$LiTaO_3$	Ilumenite	4.7	None	Hg–Q	Pure water	430	220		117, 122 (1998)
$NaTaO_3$	Perovskite	4.0	NiO	Hg–Q	Pure water	2180	1100	20 (at 270 nm)	117, 122–124 (1998)
$KTaO_3$	Perovskite	3.6	Ni	Hg–Q	Pure water	6	2		105, 117, 122 (1996)

Table 1 (*continued*)

Photocatalyst	Crystal structure	BG/eV	Co-catalyst	Light source[a]	Reactant solution	Activity/μmol h^{-1} H_2	Activity/μmol h^{-1} O_2	QY (%)	Ref. (Year)
$AgTaO_3$	Perovskite	3.4	NiO_x	Hg–Q	Pure water	21	10		125 (2002)
$KTaO_3$:Zr	Perovskite	3.6	NiO_x	Xe–Q	Pure water	9.4	4.2		126, 127 (1999)
$NaTaO_3$:La	Perovskite	4.1	NiO	Hg–Q	Pure water	19 800	9700	56 (at 270 nm)	128, 129 (2000)
$NaTaO_3$:Sr	Perovskite	4.1	NiO	Hg–Q	Pure water	9500	4700		130 (2004)
$Na_2Ta_2O_6$	Pyrochlore	4.6	NiO	Hg–Q	Pure water	391	195		131 (2006)
$K_2Ta_2O_6$	Pyrochlore	4.5	NiO	Hg–Q	Pure water	437	226		131, 132 (2004)
$CaTa_2O_6$	$CaTa_2O_6$ (orth.)	4.0	NiO	Hg–Q	Pure water	72	32		133 (1999)
$SrTa_2O_6$	$CaTa_2O_6$ (orth.)	4.4	NiO	Hg–Q	Pure water	960	490	7 (at 270 nm)	133 (1999)
$BaTa_2O_6$	$CaTa_2O_6$ (orth.)	4.1	NiO	Hg–Q	Pure water	629	303		117, 133 (1998)
$NiTa_2O_6$		3.7	None	Hg–Q	Pure water	11	4		117 (1998)
$Rb_4Ta_6O_{17}$	Layered structure	4.2	NiO	Hg–Q	Pure water	92	46		105 (1996)
$Ca_2Ta_2O_7$	Layered perovskite	4.4	NiO	Hg–Q	Pure water	170	83		131 (2006)
$Sr_2Ta_2O_7$	Layered perovskite	4.6	NiO	Hg–Q	Pure water	1000	480	12 (at 270 nm)	109–111, 134 (2000)
$K_2SrTa_2O_7$	Layered perovskite	3.9	None	Hg–Q	Pure water	374	192		135 (2004)
$RbNdTa_2O_7$	Layered perovskite	3.9	NiO_x	Hg–Q	Pure water	117	59		136–139 (1999)
$H_2La_{2/3}Ta_2O_7$	Layered perovskite	4.0	NiO_x	Hg–Q	Pure water	940	459		140 (2005)
$K_2Sr_{1.5}Ta_3O_{10}$	Layered perovskite	4.1	RuO_2	Hg–Q	Pure water	100	39.4	2 (at 252.5 nm)	141 (2007)
$LiCa_2Ta_3O_{10}$	Layered perovskite	4.2–4.3	NiO_x	Hg–Q	Pure water	708	333		142 (2008)
$KBa_2Ta_3O_{10}$	Layered perovskite	3.5	NiO_x	Hg–Q	Pure water	170		8 (<350 nm)	70 (1999)
$Sr_5Ta_4O_{15}$	Layered perovskite	4.75	NiO	Hg–Q	Pure water	1194	722		134 (2005)
$Ba_5Ta_4O_{15}$	Layered perovskite		NiO	Hg–Q	Pure water	2080	910		143 (2005)
$H_{1.8}Sr_{0.81}Bi_{0.19}Ta_2O_7$	Layered perovskite	3.88	None	Hg–Q	Pure water	250	110		144 (2008)
Mg–Ta Oxide	Mesoporous		NiO	Hg–Q	Pure water	102	51		145 (2004)
$LaTaO_4$	Fergusonite	3.9	NiO_x	Hg–Q	Pure water	116	52		146 (2001)
La_3TaO_7	Cubic fluorite	4.6	NiO_x	Hg–Q	Pure water	164	80		76, 116 (2004)
Other photocatalysts									
$PbWO_4$	Scheelite	3.9	RuO_2	Hg–Xe–Q	Pure water	24	12		147, 148 (2004)
$RbWNbO_6$	Pyrochlore	3.6	NiO_x	Hg–Q	1M RbOH	11.4	4.3		149 (2004)
$RbWTaO_6$	Pyrochlore	3.8	NiO_x	Hg–Q	1M RbOH	69.7	34.5		149 (2004)
CeO_2:Sr	Fluorite		RuO_2	Hg–Q	Pure water	110	55		150 (2007)
$BaCeO_3$	Perovskite	3.2	RuO_2	Hg–Q	Pure water	59	26		151 (2008)

[a] Hg–Q: combination of 400–450 W Hg lamp with a quartz cell, Hg–P: combination of 400–450 W Hg lamp with a Pyrex cell, Xe–Q: combination of 300–500 W Xe lamp with a quartz cell, Hg–Xe–P: combination of 1000 W Hg–Xe lamp with a Pyrex cell, Hg–Xe–Q: combination of 200 W Hg–Xe lamp with a quartz cell.

$NaCa_2Nb_3O_{10}$ and $KCa_2Nb_3O_{10}$ are active just for half reactions in the presence of sacrificial reagents.[113]

$ZnNb_2O_6$ photocatalyst with d^{10} and d^0 metal ions produce H_2 and O_2 from pure water.

Ta_2O_5 shows high activity. $K_3Ta_3Si_2O_{13}$ and $K_3Ta_3Bi_2O_{12}$ with pillared structure in which three linear chains of corner-shared TaO_6 are connected with each other are active for water splitting without any co-catalyst.[120,121] The activity of $K_3Ta_3Si_2O_{13}$ drastically increased with loading a small amount of a NiO co-catalyst while naked $K_3Ta_3B_2O_{12}$ shows high activity. Alkali and alkaline earth tantalates show photocatalytic activities for water splitting into H_2 and O_2. These tantalate photocatalysts are also active for reduction of NO_3^- to N_2 using water as an electron donor.[157]

Ishihara and co-workers have reported that photocatalytic activity of $KTaO_3$ is improved by doping of Zr, Ti and Hf. Moreover, modification of the $KTaO_3$:Zr photocatalyst by some metal complexes such as vitamin B12 improves the photocatalytic activity through a dye sensitized two-photon process.[158] On the other hand, many tantalates with layered perovskite structure are also active. The photocatalytic activity of $K_2LnTa_5O_{15}$ with tungsten bronze structure depends on Ln as well as $RbLnTa_2O_7$ with layered perovskite structure.[119,139]

Among tantalates, NiO/$NaTaO_3$ is highly active. The photocatalytic activity of NiO/$NaTaO_3$ increased remarkably with doping of lanthanide ions.[128,129] An optimized NiO (0.2 wt%)/$NaTaO_3$:La (2%) photocatalyst shows high activity with an apparent quantum yield of 56% for water splitting. The activity is stable for more than 400 h under irradiation of light from a 400-W high pressure mercury lamp. Bubbles of H_2 and O_2 evolved can be observed when the photocatalyst is irradiated with UV from a 200 W Xe–Hg lamp as shown in Fig. 15. Only light, water and photocatalyst powder exist in

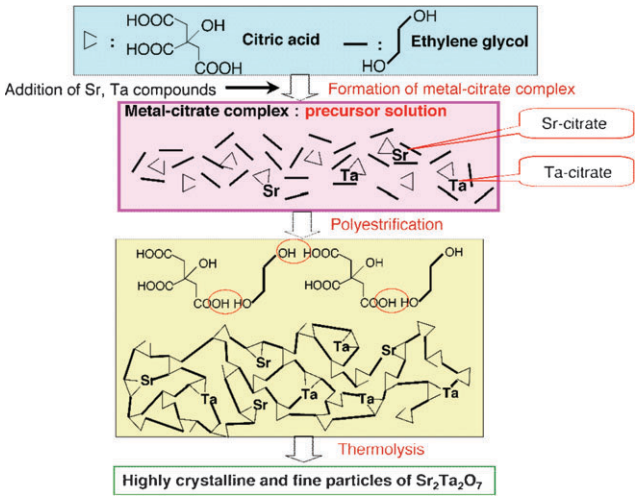

Fig. 13 Polymerizable complex method for preparation of $Sr_2Ta_2O_7$ photocatalyst.[111]

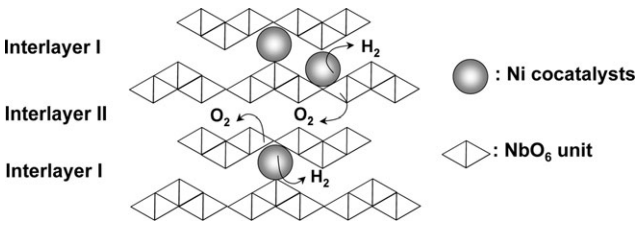

Fig. 14 Water splitting over $K_4Nb_6O_{17}$ photocatalyst with layered structure.[100]

the system. It is amazing that reduction and oxidation of water, completely opposite reactions, simultaneously proceed on the same surface of a nano-particle. The $NaTaO_3$:La photocatalyst is also active for methane coupling.[159]

A series of A_3MO_3 (A = Bi, Al, Ga and In, M = Nb and Ta) has been reported.[160,161]

5.1.3 Group 6 and other d^0 elements[147–151]. $PbWO_4$ with scheelite structure and $RbWMO_6$ (M = Nb and Ta) with pyrochlore structure are active. The f-block metal oxide, CeO_2 doped with Sr is active for water splitting, though nondoped CeO_2 is not active. The reasonable photocatalytic activity of the CeO_2:Sr is obtained using a quartz rather than a Pyrex cell even though the absorption edge of the material is around 400 nm, suggesting that excitation at higher energy than the minimum band gap excitation leads to the activity.[150]

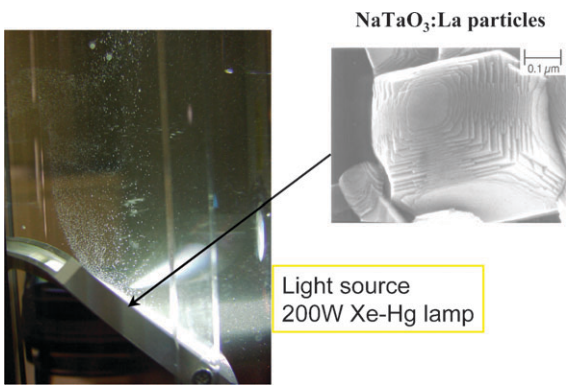

Fig. 15 Water splitting using NiO/$NaTaO_3$:La photocatalyst.

5.2 Factors affecting photocatalytic ability of d^0 metal oxides

Many photocatalysts for water splitting have been found as shown in Table 1. It is important to make such a photocatalyst library because the relationship between the nature of materials and the photocatalytic abilities can be considered. For example, systematic comparison of photocatalytic activities between niobates and tantalates with similar structure give some information on factors that affect photocatalytic ability as mentioned below.

5.2.1 Effect of conduction band level consisting of Nb 4d and Ta 5d orbitals on photocatalytic performances[109]. $Sr_2Nb_2O_7$ possesses a layered perovskite structure that is the same as $Sr_2Ta_2O_7$ though the distortion of the framework is slightly different as shown in Fig. 16.[162,163] These crystal structures are composed of NbO_6 and TaO_6 octahedra. Moreover, the ionic radius of Nb^{5+} is almost the same as that of Ta^{5+}. However, the photocatalytic activity of $Sr_2Ta_2O_7$ is higher than that of $Sr_2Nb_2O_7$ as shown in Table 1 even if the number of absorbed photons of $Sr_2Ta_2O_7$ should be smaller than that of $Sr_2Nb_2O_7$ under the same experimental condition, because the band gap of the former is wider than that of the latter. The difference in photocatalytic activities between niobates and tantalates is mainly due to the conduction band level. The conduction band of $Sr_2Ta_2O_7$ consists of Ta 5d while that of $Sr_2Nb_2O_7$ is Nb 4d. The valence band potential of $Sr_2Ta_2O_7$ should be similar to that of $Sr_2Nb_2O_7$ because the valence bands consist of O 2p orbitals and six oxygen anions coordinate to Ta^{5+} or Nb^{5+} with the same ionic radius. Eqn (11), as reported by Scaife for oxides not containing metal cations with partly filled d orbital can be applied to the present system for the approximate determination of the flat band potential,[164] where V_{fb} and E_g represent a flat band potential and a band gap, respectively.

$$V_{fb}(\text{NHE}) = 2.94 - E_g \qquad (11)$$

The band structures of $Sr_2Ta_2O_7$ and $Sr_2Nb_2O_7$ can be roughly described as shown in Fig. 17.[109] Band structure of NiO is also shown.[165] O_2 evolution on $Sr_2Ta_2O_7$ is as easy as that on $Sr_2Nb_2O_7$ because the potentials of their valence bands are deep enough to oxidize water into O_2. Therefore, it is due to the difference in the conduction band level that the

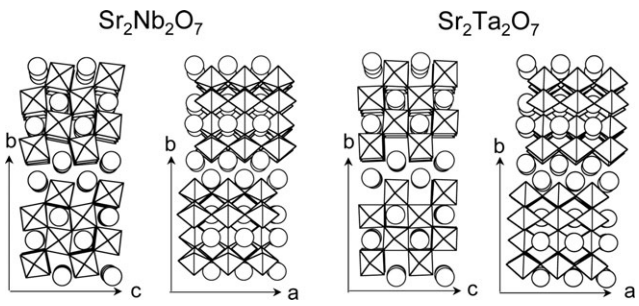

Fig. 16 Layered perovskite structures of $Sr_2M_2O_7$ (M = Nb and Ta).[162,163]

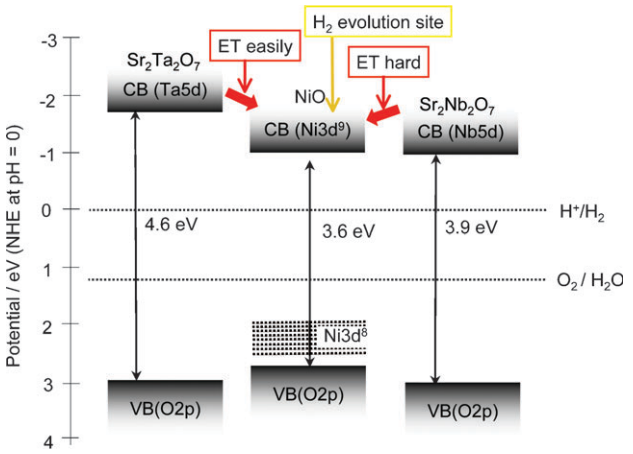

Fig. 17 Band structures of $Sr_2M_2O_7$ (M = Nb and Ta) photocatalysts and NiO co-catalyst.[109]

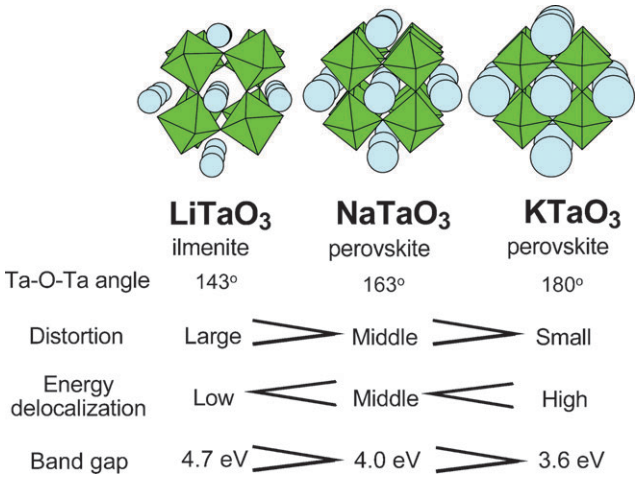

Fig. 18 Crystal and energy structures of alkali tantalate photocatalysts.[122]

photocatalytic activity of $Sr_2Ta_2O_7$ is higher than that of $Sr_2Nb_2O_7$. The high conduction band level causes the driving force for reduction of water to form H_2. The reason why $Sr_2Ta_2O_7$ is able to decompose pure water without co-catalysts is also due to its high conduction band.

In general, pretreatment of H_2 reduction and subsequent O_2 oxidation is indispensable for obtaining high activities for NiO-loaded photocatalysts as mentioned in section 5.1.1. The pretreatment is indispensable for $NiO/Sr_2Nb_2O_7$ as usual whereas it is not for $NiO/Sr_2Ta_2O_7$. In the case of the non-treated $NiO/Sr_2Ta_2O_7$ photocatalyst, it is possible that the photogenerated electrons in a conduction band of $Sr_2Ta_2O_7$ can transfer to a conduction band of NiO because of the suitable potential difference as shown in Fig. 17. In contrast, this appears to be difficult for $Sr_2Nb_2O_7$ because the potential difference in the conduction band between $Sr_2Nb_2O_7$ and NiO is negligible. In such a case, pretreatment would be necessary as well as in the case of $NiO/SrTiO_3$. Therefore, the effect of the conduction band level dominates the photocatalytic activities of the $Sr_2M_2O_7$ system. Systematic investigation of solid solutions also gives some information on factors affecting photocatalytic activities.[110,111]

In this section, main factors were just discussed from the viewpoint of band structure as shown in Fig. 5. The nature of connection of MO_6 octahedra in crystal structure should be suitable for migration of photogenerated electrons and holes, and surface reactions of the carriers with water as indicated by steps (ii) and (iii) in Fig. 4 as mentioned in the next section.

5.2.2 Effect of distortion of framework of crystal structure on energy structure[109,122]. All of $ATaO_3$ (A: Li, Na, and K) consist of corner-sharing TaO_6 octahedra with perovskite-like structures as shown in Fig. 18.[122] The photocatalytic activities of $ATaO_3$ depends on the A site cation of perovskite-like structure. The bond angles of Ta–O–Ta are 143° ($LiTaO_3$), 163° ($NaTaO_3$) and 180° ($KTaO_3$) in octahedral connection. Wiegel and co-workers have reported the relationship between crystal structures and energy delocalization for alkali tantalates $ATaO_3$ (A: Li, Na, and K).[166] As the bond angle approaches 180°, excited energy or electron–hole pairs in the crystal migrate more easily and the band gap becomes narrower. Therefore, the order of the delocalization of excited energy or electron–hole pairs is $LiTaO_3$ < $NaTaO_3$ < $KTaO_3$, while that of the band gap is reversed in the order. The degree of localization affects the step (ii) in Fig. 4. This discussion is applied to other photocatalyst systems.[109,125,167] $NaTaO_3$ shows the highest photocatalytic activity among the $ATaO_3$ (A: Li, Na, and K) photocatalysts when a NiO co-catalyst is loaded. In the case of $NaTaO_3$, excess sodium in the starting material is indispensable for showing the high activity indicating that preparation conditions are important.[123] The conduction band level of the $NaTaO_3$ photocatalyst is higher than that of NiO[165] as shown in Fig. 19.[122] Moreover, the excited energy is delocalized in the $NaTaO_3$ crystal. Therefore, the photogenerated electrons in the conduction band of the $NaTaO_3$ photocatalyst are able to transfer to the conduction band of the NiO co-catalyst. Therefore, NiO-loading is effective for the $NaTaO_3$ photocatalyst even without special pretreatment as observed for a $NiO/Sr_2Ta_2O_7$ photocatalyst. Thus, the high activity of $NiO/NaTaO_3$ is due to the suitable conduction band level consisting of Ta 5d and energy delocalization caused by the small distortion of TaO_6 connections.

Charge separation of photogenerated electrons and holes is required in the case of a water splitting reaction into H_2 and O_2 more strongly than in the case of photocatalytic reactions

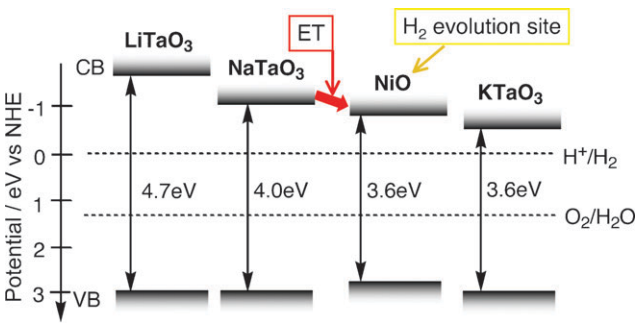

Fig. 19 Band structures of alkali tantalate photocatalysts and NiO co-catalyst.[122]

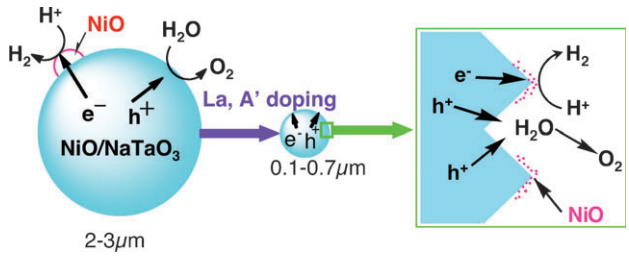

Fig. 20 Mechanism of highly efficient water splitting over NiO/$NaTaO_3$:La photocatalyst.[129]

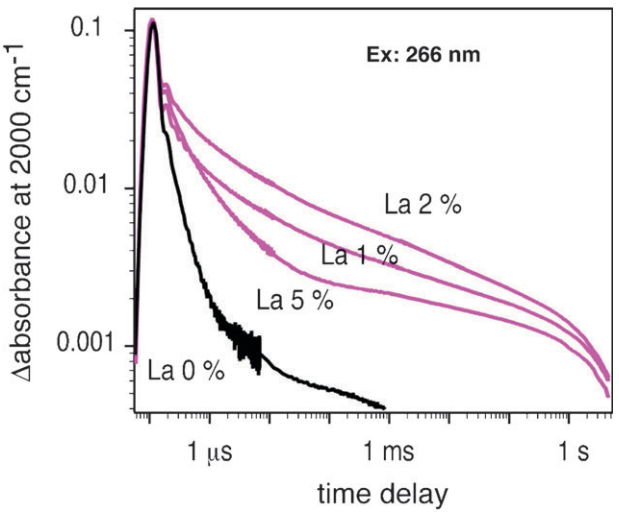

Fig. 21 Decay curves of photogenerated electrons in La-doped $NaTaO_3$.[168]

in the presence of sacrificial reagents in order to prevent recombination. $Sr_2Nb_2O_7$ has a dipole moment along perovskite layers, the *c* axis, due to the distortion of the framework of perovskite layers as shown in Fig. 16. The charge separation may be enhanced by the dipole moment.[109] Inoue has proposed the effects of local distortion of polyhedra consisting of the crystal structure of photocatalysts on the charge separation.[18] These factors affect charge separation of the step (ii) in Fig. 4.

5.2.3 Effect of morphology on creation of active sites[128–130].

The photocatalytic activity of NiO/$NaTaO_3$ increases remarkably with doping of La ions.[128,129] The reaction scheme for the water splitting on the NiO/$NaTaO_3$:La photocatalyst is shown in Fig. 20.[129] The particle size of the $NaTaO_3$:La crystal (0.1–0.7 μm) is smaller than that of the nondoped $NaTaO_3$ crystal (2–3 μm) and ordered surface nano-steps are created by lanthanum doping. The small particle size with high crystallinity is advantageous in terms of increasing the probability of the reactions of photogenerated electrons and holes with water molecules, rather than recombination as shown in Fig. 7. The H_2 evolution site of the edge is effectively separated from the O_2 evolution site of the groove at the surface nanostep structure. This separation is advantageous, especially for water splitting in order to avoid the back reaction. Doping of Ca, Sr and Ba also gives the same effect as the La doping on the formation of the characteristic morphology of $NaTaO_3$ and the improvement of photocatalytic activity.[130] Thus, the change in surface morphology affects the step (iii) in Fig. 4.

Time-resolved IR measurements reveal that the La doping prolongs the lifetime of photogenerated electrons in a conduction band or a shallow trap level as shown in Fig. 21.[168] The absorption is due to the electrons photogenerated by band gap excitation at 266 nm. The increase in the lifetime is also one of the factors for the improvement of photocatalytic ability. This factor affects the step (ii) in Fig. 4.

5.3 Oxide photocatalysts consisting of d^{10} metal cations[169–180]

d^{10} metal oxides such as ZnO and In_2O_3 are well-known photocatalysts for a long time. However, they are not active for water splitting because of photocorrosion according to eqn (5) and the low conduction band level, respectively.[7] In contrast, Inoue's group has found various mixed oxide photocatalysts consisting of d^{10} metal cations, Ga^{3+}, In^{3+}, Ge^{4+}, Sn^{4+} and Sb^{5+}, for water splitting as shown in Table 2.

Table 2 Oxide photocatalysts based on d^{10} metal ions for water splitting under UV irradiation[a]

			Activity/μmol h^{-1}		
Photocatalyst	Crystal structure	BG[d]/eV	H_2	O_2	Ref. (Year)
$NaInO_2$	Layered structure	3.9	0.9	0.3	169, 170 (2003)
$CaIn_2O_4$	Tunnel structure		21	10	169–172 (2001)
$SrIn_2O_4$	Tunnel structure	3.6	7	3	169–173 (2001)
$LaInO_3$		4.1	1	0.5	172 (2003)
$Y_xIn_{2-x}O_3$		4.3	8	4	174 (2008)
$NaSbO_3$	Ilmenite	3.6	1.7	0.8	171, 175 (2001)
$CaSb_2O_6$	Layered structure	3.6	1.5	0.2	175 (2002)
$Ca_2Sb_2O_7$	Weberite	3.9	3	1	175 (2002)
$Sr_2Sb_2O_7$	Weberite	4.0	8	3	175 (2002)
Sr_2SnO_4			5	2.5	171 (2001)
$ZnGa_2O_4$		4.2	10	4	176 (2002)
Zn_2GeO_4	Willemite	4.6	22	10	177 (2004)
$LiInGeO_4$		4.4	26	13	178 (2005)
Ga_2O_3[b]		4.6	46	23	179 (2004)
Ga_2O_3:Zn[c]		4.6	4100	2200	180 (2008)

[a] Co-catalyst: RuO_2, reactant solution: pure water, light source: 200 W Hg–Xe lamp and a quartz cell. [b] Co-catalyst: NiO, light source: 450 W Hg lamp equipped in a quartz cell. [c] Co-catalyst: Ni, light source: 450 W Hg lamp equipped in a quartz cell. [d] Band gaps not mentioned in papers were determined from DRS.

A RuO_2 co-catalyst is indispensable for these photocatalysts except for a Ga_2O_3 photocatalyst. The RuO_2 co-catalyst is loaded using $Ru_3(CO)_{12}$ by an impregnation method. Conduction bands of these photocatalysts consist of sp orbitals of d^{10} metal cations. These bands are dispersed well resulting in high mobility of photogenerated electrons. Inoue has proposed that the dipole moment formed by distortions of MO_4 tetrahedra and MO_6 octahedra enhances charge separation of photogenerated carriers.[170,176,177] The $CaIn_2O_4$ photocatalyst is also used for degradation of Methylene Blue.[181–184] Sakata and co-workers have reported a highly efficient Zn-doped β-Ga_2O_3 photocatalyst with a Ni co-catalyst.[180]

6. Wide band gap metal oxide photocatalysts for H_2 or O_2 evolution from an aqueous solution containing a sacrificial reagent under UV irradiation[185–197]

Many metal oxide photocatalysts for water splitting without any sacrificial reagents have been developed as shown in Tables 1 and 2. Therefore, it may appear meaningless to develop wide band gap metal oxide photocatalysts not for water splitting but for H_2 or O_2 evolution from an aqueous solution containing a sacrificial reagent under UV irradiation. However, their development is still important to get information on factors affecting photocatalytic activity.

Table 3 shows wide band gap metal oxide photocatalysts that are active for H_2 or O_2 evolution from an aqueous solution containing a sacrificial reagent under UV irradiation.

Many layered titanates are active for H_2 evolution. H^+-exchange often gives higher activity for H_2 evolution than the native materials even in the absence of co-catalysts such as Pt. It means that these protonated layered metal oxides possess excellent active sites for H_2 evolution. $K_2Ti_4O_9$ and $HCa_2Nb_3O_{10}$ with SiO_2 pillars at the interlayer show high activities.[188] These layered metal oxides are attractive materials for preparing nano-sheets. Sasaki's group has extensively studied nano-sheets of layered oxide materials,[198] and the term "nano-sheet" was probably first used by Sasaki's group. Titanate nano-sheets show photocatalytic activity for self-cleaning. Osterloh and co-workers have reported photocatalytic reactions using $Pt/HCa_2Nb_3O_{10}$ nano-sheets.[199,200]

Table 3 Oxide photocatalysts for H_2 or O_2 evolution from aqueous solutions in the presence of sacrificial reagents under UV irradiation

				H_2 evolution[b]		O_2 evolution[c]	
Photocatalyst	Crystal structure	BG/eV	Light source[a]	Co-catalyst	Activity/μmol h^{-1}	Activity/μmol h^{-1}	Ref. (Year)
$Na_2Ti_3O_7$	Layered structure		Xe–P	Pt	19	—	185 (1987)
$K_2Ti_2O_5$	Layered structure		Xe–P	Pt	34.7	—	185 (1987)
$K_2Ti_4O_9$	Layered structure		Xe–P	Pt	4.8	—	185 (1987)
$Cs_2Ti_2O_5$	Layered structure	4.4	Hg–Q	None	500	—	186 (1997)
H^+-$Cs_2Ti_2O_5$	Layered structure		Hg–Q	None	852	—	186 (1997)
$Cs_2Ti_5O_{11}$	Layered structure	3.75	Hg–Q	None	90	—	186 (1997)
$Cs_2Ti_6O_{13}$	Layered structure	3.7	Hg–Q	None	38	—	186 (1997)
H^+-$CsTiNbO_5$	Layered structure	3.0	Hg–P	Pt	87	—	187 (1990)
H^+-$CsTi_2NbO_7$	Layered structure	3.2	Hg–P	Pt	320	—	187 (1990)
SiO_2-pillared $K_2Ti_4O_9$	Layered structure	3.17	Hg–P	Pt	560	—	188 (2000)
SiO_2-pillared $K_2Ti_{2.7}Mn_{0.3}O_7$	Layered structure		Hg–P	None	320	—	188 (2000)
$Na_2W_4O_{13}$	Layered structure	3.1	Hg–P	Pt	21	9	189 (1997)
H^+-$KLaNb_2O_7$	Layered perovskite		Hg–Q	Pt	3800	46	8 (2000)
H^+-$RbLaNb_2O_7$	Layered perovskite		Hg–Q	Pt	2600	2	8 (2000)
H^+-$CsLaNb_2O_7$	Layered perovskite		Hg–Q	Pt	2200	3	8 (2000)
H^+-$KCa_2Nb_3O_{10}$	Layered perovskite		Hg–Q	Pt	19 000	8	8 (2000)
SiO_2-pillared $KCa_2Nb_3O_{10}$	Layered perovskite		Hg–P	Pt	10 800		190, 191 (1993)
ex-$Ca_2Nb_3O_{10}/K^+$ nanosheet[4)]	Layered perovskite		Xe–P	Pt	550		192 (2002)
Restacked ex-$Ca_2Nb_3O_{10}/Na^+$	Layered perovskite		Xe–P	Pt	880		192 (2002)
H^+-$RbCa_2Nb_3O_{10}$	Layered perovskite		Hg–Q	Pt	17 000	16	8 (2000)
H^+-$CsCa_2Nb_3O_{10}$	Layered perovskite		Hg–Q	Pt	8300	10	8 (2000)
H^+-$KSr_2Nb_3O_{10}$	Layered perovskite		Hg–Q	Pt	43 000	30	8 (2000)
H^+-$KCa_2NaNb_4O_{13}$	Layered perovskite		Hg–Q	Pt	18 000	39	8 (2000)
$Bi_2W_2O_9$	Aurivillius like	3.0	Hg–P	Pt	18	281	193 (1999)
$Bi_2Mo_2O_9$	Aurivillius like	3.1	Xe–P	—	—	1.8	193 (1999)
$Bi_4Ti_3O_{12}$	Aurivillius	3.1	Hg–P	Pt	0.6	3	193 (1999)
$BaBi_4Ti_4O_{15}$	Aurivillius	3.1	Hg–P	Pt	8.2	3.7	193 (1999)
Bi_3TiNbO_9	Aurivillius	3.1	Hg–P	Pt	33	31	193 (1999)
$PbMoO_4$	Scheelite	3.31	Xe–P	Pt	1.9	12.8	194 (1990)
$(NaBi)_{0.5}MoO_4$	Scheelite	3.1	Xe–P	Pt	0.6	58	195 (2004)
$(AgBi)_{0.5}MoO_4$	Scheelite	3.0	Xe–P	Pt	0	10.7	195 (2004)
$(NaBi)_{0.5}WO_4$	Scheelite	3.5	Xe–P	Pt	7	1.3	195 (2004)
$(AgBi)_{0.5}WO_4$	Scheelite	3.5	Xe–P	Pt	0.1	5.8	195 (2004)
$Ga_{1.14}In_{0.86}O_3$		3.7	Hg–P	Pt	30	30	196 (1998)
β–Ga_2O_3		4.6	Xe–Q	Pt	50	7	196 (1998)
$Ti_{1.5}Zr_{1.5}(PO_4)_4$		3.8	Xe–Q	Pt	11.8	—	197 (2005)

[a] Hg–Q: combination of 400–450 W Hg lamp with a quartz cell, Hg–P: combination of 400–450 W Hg lamp with a Pyrex cell, Xe–Q: combination of 300 W Xe lamp with a quartz cell, Xe–P: combination of 300 W Xe lamp with a quartz cell. [b] Sacrificial reagent: CH_3OH aq. [c] Sacrificial reagent: $AgNO_3$ aq. [d] ex-$Ca_2Nb_3O_{10}/K^+$ means that nanosheet was flocculated with K^+.

$Bi_2W_2O_9$, $BaBi_4Ti_4O_{15}$ and Bi_3TiNbO_9 consisting of a layered structure with perovskite slabs are active not only for O_2 but also H_2 evolution in the presence of sacrificial reagent. $Na_2W_4O_{13}$ photocatalyst with layered structure is also active for H_2 or O_2 evolution from aqueous solutions in the presence of sacrificial reagents although WO_3 is inactive for H_2 evolution. Homogeneous photocatalysts of tungsten-polyacids are also active for H_2 evolution.[201]

$PbMoO_4$ with scheelite structure shows activities for H_2 and O_2 evolution in the presence of sacrificial reagents under UV irradiation. The substituted compounds, $Na_{0.5}Bi_{0.5}MoO_4$, $Ag_{0.5}Bi_{0.5}MoO_4$, $Na_{0.5}Bi_{0.5}WO_4$ and $Ag_{0.5}Bi_{0.5}WO_4$, are also active for O_2 evolution. In these photocatalysts, although these molybdates and tungstates respond to only UV, Pb, Bi and Ag play an important role for making the valence bands as mentioned in section 7.1.4.

Solid solutions of β-Ga_2O_3 and In_2O_3 consisting of d^{10} cations have been systematically studied for photocatalytic activities for H_2 or O_2 evolution from aqueous solutions in the presence of sacrificial reagents.[196] In this photocatalyst system, the band gap and luminescent energy decrease as the ratio of indium increases.

7. Photocatalysts with visible light response for H_2 or O_2 evolution from an aqueous solution containing a sacrificial reagent

Development of photocatalysts that work only for half reactions of water splitting in the presence of sacrificial reagents might seem meaningless but this view is incorrect. These photocatalysts can be used to construct *Z*-scheme systems that are active for water splitting under visible light irradiation as mentioned in section 8.3. Moreover, some of them will be able to produce H_2 using biomass and abundant compounds.[33–38] Tables 4 and 5 list photocatalysts for H_2 or O_2 evolution from aqueous solutions containing sacrificial reagents under visible light irradiation.

7.1 Oxide photocatalysts[4–5,125,193,202–231]

7.1.1 Design of oxide photocatalysts with visible light response. Suitable band engineering is required in order to develop new photocatalysts for water splitting under visible light irradiation as shown in Fig. 22. In general, the conduction bands of stable oxide semiconductor photocatalysts are composed of empty orbitals (LUMOs) of metal cations with d^0 and d^{10} configurations. Although the valence band level depends on crystal structure and bond character between metal and oxygen, the level of the valence band consisting of O 2p orbitals is usually *ca.* 3.0 eV.[164] Accordingly, a new valence band or an electron donor level (DL) must be formed with orbitals of elements other than O 2p to make the band gap (BG) or the energy gap (EG) narrower because the conduction band level should not be lowered. Not only the thermodynamic potential but also kinetic ability for 4-electron oxidation of water are required for the newly formed valence band. Strategies for the band engineering are shown in Fig. 23. The electron donor level is created above a valence band by

Table 4 Oxide photocatalysts for H_2 or O_2 evolution from aqueous solutions in the presence of sacrificial reagents under visible light irradiation

			Activity/μmol h^{-1}		
Photocatalyst	BG (EG)/eV	Light source[a]	H_2[b]	O_2[c]	Ref. (Year)
WO_3	2.8	Xe–L42	—	65	4, 5, 202–204 (1962)
Bi_2WO_6	2.8	Xe–L42	—	3	193 (1999)
Bi_2MoO_6	2.7	Xe–L42	—	55	205 (2006)
$Bi_2Mo_3O_{12}$	2.88	Xe–L42	—	8	205 (2006)
$Zn_3V_2O_8$	2.92	Xe–L42	—	10.2	206 (2005)
$Na_{0.5}Bi_{1.5}VMoO_8$	2.5	Xe–L42	—	74	207 (2008)
$In_2O_3(ZnO)_3$	2.6	Xe–L42	1.1	1.3	208 (1998)
$SrTiO_3$:Cr/Sb	2.4	Xe–L42	78	0.9	209 (2002)
$SrTiO_3$:Ni/Ta	2.8	Xe–L42	2.4	0.5	210 (2005)
$SrTiO_3$:Cr/Ta	2.3	Xe–L42	70	—	211 (2004)
$SrTiO_3$:Rh	2.3	Xe–L42	117	0	212 (2004)
$CaTiO_3$:Rh		Xe–L42	8.5	0	213 (2006)
$La_2Ti_2O_7$:Cr	2.2	Hg–L42	15	—	214, 215 (2004)
$La_2Ti_2O_7$:Fe	2.6	Hg–L42	10	—	214, 215 (2004)
TiO_2:Cr/Sb	2.2	Xe–L42	0.06	31.5	209 (2002)
TiO_2:Ni/Nb	2.6	Xe–L44	0	7.6	210 (2005)
TiO_2:Rh/Sb	2.13	Xe–L44	—	16.9	216 (2007)
$PbMoO_4$:Cr	2.26	Xe–L42	—	71.5	217 (2007)
$RbPb_2Nb_3O_{10}$	2.5	Xe–L42	4	1.1	218 (1993)
$PbBi_2Nb_2O_9$	2.88	W–L42	3.2	520	219, 220 (2004)
$BiVO_4$	2.4	Xe–L42	—	421	221–224 (1998)
$BiCu_2VO_6$	2.1	Xe–L42	—	2.3	225 (2005)
$BiZn_2VO_6$	2.4	Xe–L42	—	6	226 (2006)
$SnNb_2O_6$	2.3	Xe–L42	14.4	62.8[d]	227–229 (2004)
$AgNbO_3$	2.86	Xe–L42	8.2	37	125 (2002)
Ag_3VO_4	2.0	Xe–L42	—	17	230 (2003)
$AgLi_{1/3}Ti_{2/3}O_2$	2.7	Xe–L42	—	24	231 (2008)
$AgLi_{1/3}Sn_{2/3}O_2$	2.7	Xe–L42	—	53	231 (2008)

[a] Xe–L42: 300–500 W Xe lamp with a cut-off filter (L42), Hg–L42: 500 W lamp with a cut-off filter (L42), Xe–L44: 300 W Xe lamp with a cut-off filter (L44), W–L42: 450 W lamp with a cut-off filter (L42). [b] Co-catalyst: Pt, sacrificial reagent: CH_3OH aq. [c] Sacrificial reagent: $AgNO_3$ aq. [d] Co-catalyst: IrO_2.

Table 5 Dye sensitized photocatalysts for H_2 evolution from aqueous solutions in the presence of sacrificial reagents under visible light irradiation

Photocatalyst	Sensitizer	Sacrificial reagent	Light source	Incident light/nm	H_2 evolution/μmol h^{-1}	Ref. (Year)
TiO_2	$Ru(bpy)_3^{2+}$	Water–MeOH vapor	500 W Xe	>440	0.9	270, 271 (1982)
Pt/ZnO	Erythrosine	Triethanolamine + I^-	500 W Xe	>420	80.4	272 (1985)
$H_2K_2Nb_6O_{17}$	$Ru(bpy)_3^{2+}$	I^-	500 W Hg–Xe	>400	0.4	273 (1993)
Pt/TiO_2	Zn-porphyrin	EDTA	1000 W Xe	>520	182 (9h)[a]	274 (1995)
Pt/TiO_2	NK-2405	Acetonitrile + I	300 W Xe	>410	210	275, 276 (2003)
Pt/TiO_2	C-343	Acetonitrile + I	300 W Xe	>410	156	275, 276 (2003)
$Pt(in)/H_4Nb_6O_{17}$	NK-2405	Acetonitrile + I	300 W Xe	>410	94	275, 276 (2003)
$Ni/K_4Nb_6O_{17}$	CdS	K_2SO_3	300 W Xe	>420	56	277, 278 (1988)
$H_4Nb_6O_{17}$	CdS	Na_2S	100 W Hg	>400	220	279 (2001)
$H_2Ti_4O_9$	CdS	Na_2S	100 W Hg	>400	560	279 (2001)

[a] Turnover number.

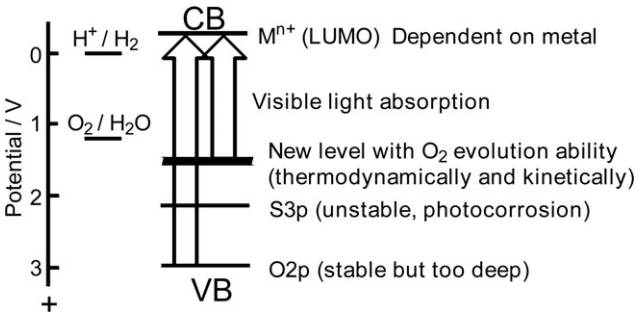

Fig. 22 Band structure control to develop visible light-driven-photocatalysts for water splitting.

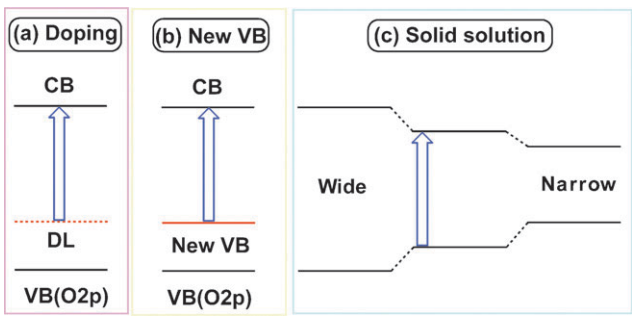

Fig. 23 Strategies of band engineering for design of visible-light-driven photocatalysts.

doping some elements into conventional photocatalysts with wide band gaps such as TiO_2 and $SrTiO_3$. It results in the formation of energy gap. On the other hand, some metal cations and anions can contribute to valence band formations above the valence band consisting of O 2p orbitals. Here, band gap is distinguished from energy gap. The energy gap is formed by the impurity level that does not form a complete band. Making a solid solution is also a useful band engineering procedure. Such band engineering is related to the step (i) in Fig. 4.

Oxide photocatalysts for H_2 or O_2 evolution from aqueous solutions in the presence of sacrificial reagents under visible light irradiation are summarized in Table 4.

7.1.2 Native visible-light driven photocatalysts[193,202–208]. WO_3 is one of the most well known photocatalysts with visible light response for O_2 evolution in the presence of sacrificial reagents such as Ag^+ and Fe^{3+}. Abe and co-workers recently found that Pt/WO_3 is active for degradation of acetic acid, CH_3CHO and IPA under visible light irradiation.[232]

Bi_2WO_6 and Bi_2MoO_6 with the Aurivillius structure are active for an O_2 evolution reaction under visible light irradiation. These tungstate and molybdate photocatalysts are not active for H_2 evolution because of the low conduction band level. These photocatalysts are also used for degradation of HCHO,[233] CH_3OH,[234] CH_3COOH,[235,236] Rhodamine B[237–249] and Methylene Blue.[240,244,247]

7.1.3 Doped photocatalysts[209–217]. Doping has often been attempted to prepare visible light-driven photocatalysts (Fig. 23(a)). Here, doping often means replacement with a foreign element at a crystal lattice point of the host material. A TiO_2 photocatalyst is usually employed as a host material for the doping. However, although the white powder becomes colored with doping of transition metal cations, in general, the photocatalytic activity drastically decreases because of formation of recombination centres between photogenerated electrons and holes, even under band gap excitation. However, doping of transition metals is a good strategy to develop visible light responsive photocatalysts if a suitable dopant is chosen as mentioned below.

Co-doping of Cr^{3+}/Ta^{5+}, Cr^{3+}/Sb^{5+}, Ni^{2+}/Ta^{5+} and doping of Rh cations is effective in sensitization of $SrTiO_3$ to visible light. These doped $SrTiO_3$ powders with Pt co-catalysts show photocatalytic activities for H_2 evolution from aqueous methanol solutions under visible light irradiation. Cr and Fe are effective dopants for H_2 evolution over a $La_2Ti_2O_7$ photocatalyst. Rh-doped $SrTiO_3$ is one of the rare oxide photocatalysts that can efficiently produce H_2 under visible light irradiation. This Rh doping is also effective for $CaTiO_3$. The $SrTiO_3$:Rh photocatalyst plays an important role on a *Z*-scheme photocatalyst system for water splitting under visible light irradiation as mentioned in section 8.3. On the other hand, TiO_2 (rutile) co-doped with Cr^{3+}/Sb^{5+}, Rh^{3+}/Sb^{5+} and Ni^{2+}/Nb^{5+} is active for O_2 evolution from aqueous silver nitrate solutions. In these doped photocatalysts, the dopants form electron donor levels in the band gap of the TiO_2 and $SrTiO_3$ host materials, resulting in visible light response. When Ti^{4+} is replaced with Cr^{3+} or Ni^{2+}, the charge becomes unbalanced. This may result in the formation of recombination centres. Co-doped metal cations such as Nb^{5+}, Ta^{5+} and Sb^{5+} compensate the charge imbalance, resulting in the suppression of the formation of the

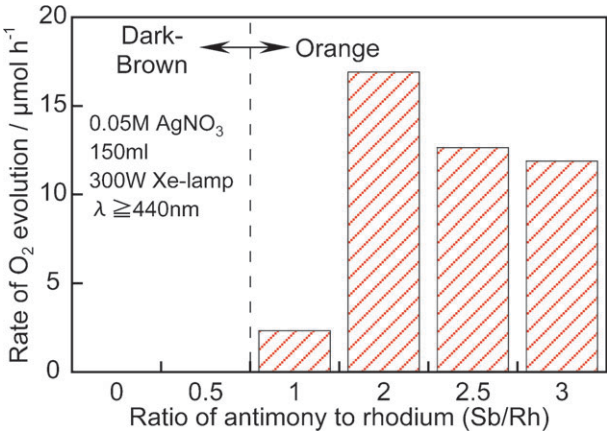

Fig. 24 Effect of co-doping of Sb to TiO_2:Rh (1.3%) on photocatalytic activity under visible light irradiation.[216]

recombination centres and maintaining the property of visible light absorption. When about 1% of Cr was doped into TiO_2 without any co-dopant, activities were never obtained as a rule. Thus, transition metal doping into photocatalysts with wide band gaps is effective for the development of visible light responsive photocatalysts if a suitable combination of dopant–co-dopant is chosen. Next, the co-doping effect is discussed using the TiO_2:Rh/Sb and TiO_2:Cr/Sb photocatalysts in more detail.

Fig. 24 shows dependence of photocatalytic O_2 evolution from an aqueous silver nitrate solution on TiO_2:Rh/Sb upon the ratio of doped Sb to Rh.[216] When only Rh is doped into TiO_2 no activity is obtained and the colour of the photocatalyst is black. When the ratio of Sb/Rh is equal to or larger than the unity O_2 evolution activity is observed accompanied with a colour change from black to orange. TiO_2:Rh without co-doping of Sb contains Rh^{4+} because Rh is doped at a Ti^{4+} site. The Rh^{4+} species predominantly works as a recombination site. As the ratio of co-doped Sb increases, the formation of Rh^{4+} is suppressed. Co-doping with Sb^{5+} produces Rh^{3+} forming an electron donor level, due to keeping of the charge balance, and results in showing of photocatalytic activities. The same dependency is observed for a TiO_2:Cr/Sb photocatalyst in which formation of Cr^{6+} is suppressed by the Sb^{5+} co-doping.[209] It is confirmed by IR transient absorption spectroscopy for the TiO_2:Cr/Sb photocatalyst that the Sb^{5+} co-doping prolongs a lifetime of photogenerated electrons as shown in Fig. 25.[251] TiO_2:Cr/Sb with 1.0–2.0 of optimum ratios gives slowest decay when it is excited by 532 nm. It is interesting that the lifetime of photogenerated electrons for the optimized TiO_2:Cr/Sb is longer than that for nondoped TiO_2 even by the band gap excitation. The decay is too fast to measure in this time scale by pumping of both wavelengths for inactive TiO_2:Cr/Sb with smaller ratios than unity. The visible light responses are due to the transitions from electron donor levels consisting of Rh^{3+} and Cr^{3+} to the conduction band of the TiO_2 host. The TiO_2:Rh/Sb and TiO_2:Cr/Sb photocatalysts can use visible light up to 600 nm, of relatively long wavelength for O_2 evolution photocatalysts.

$PbMoO_4$ shows activities for H_2 and O_2 evolution in the presence of sacrificial reagents under UV irradiation as shown in Table 3. When Cr^{6+} is partly replaced for Mo^{6+} in this host material Cr^{6+} forms an electron acceptor level resulting in a visible light response.[217] DFT calculation revealed that this visible light response is due to the transition from the valence band consisting of Pb 6s and O 2p to the electron acceptor level composed of Cr 3d empty orbitals. Formation of such an acceptor level is also useful for sensitization of wide band gap photocatalysts to visible light if the potential for H_2 evolution is not required.

Anion doping such as nitrogen to a TiO_2 photocatalyst has been studied for oxidation of organic compounds.[250]

7.1.4 Valence band-controlled photocatalysts[218–231]. In the doped photocatalysts mentioned above, the formation of recombination sites by the dopant is more or less inevitable. Moreover, the level formed by the dopant is usually discrete and thus inconvenient for the migration of holes formed there. Therefore, the formation of a valence band by orbitals not associated with O 2p but with other elements is indispensable for oxide photocatalysts in order to design visible light-driven photocatalysts (Fig. 23(b)).

Orbitals of Pb 6s in Pb^{2+}, Bi 6s in Bi^{3+}, Sn 5s in Sn^{2+} and Ag 4d in Ag^{+} can form valence bands above the valence band

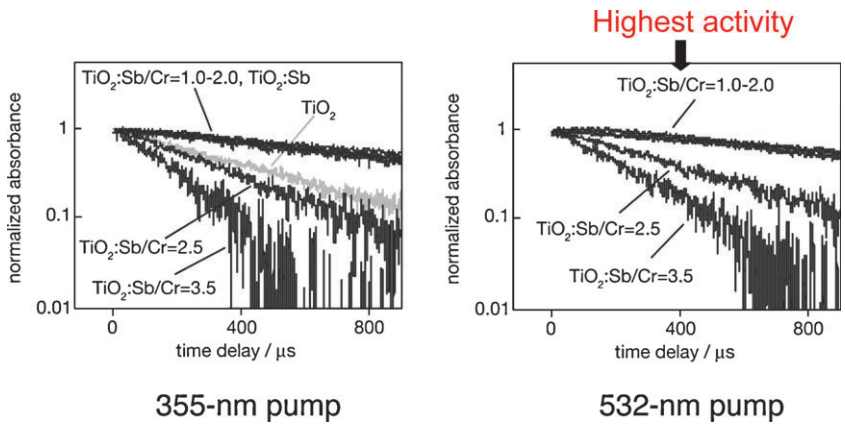

Fig. 25 Decay curves of photogenerated electrons in TiO_2:Sb/Cr photocatalyst.[251]

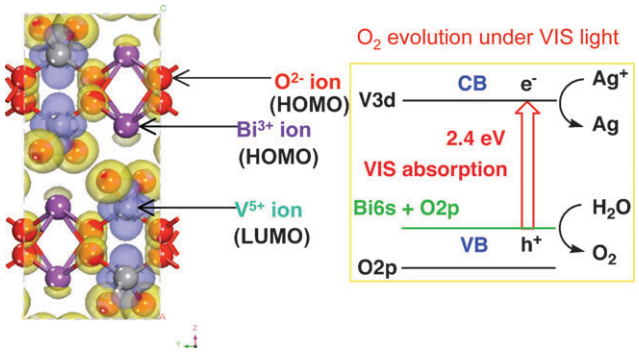

Fig. 26 Band structure of $BiVO_4$ calculated by DFT.

consisting of O 2p orbitals in metal oxide photocatalysts. The degree of the contribution of these metal cations to the valence band formation depends on the crystal structure and the ratio of the metal cations contained.

$RbPb_2Nb_3O_{10}$ and $PbBi_2Nb_2O_9$ with layered perovskite structure show activity for H_2 or O_2 evolution.

$BiVO_4$ with a monoclinic scheelite structure shows photocatalytic activities for O_2 evolution from aqueous silver nitrate solutions under visible light irradiation. $BiVO_4$ can be prepared by an aqueous process at ambient temperature and pressure[222,223] in an environmentally friendly process. The photocatalytic activity of $BiVO_4$ prepared by the aqueous process is much higher than that of $BiVO_4$ prepared by a conventional solid state reaction. The difference in the photocatalytic activity between $BiVO_4$ obtained by the different methods is due to the crystallinity and defects. The aqueous process is especially advantageous for the preparation of materials in which defects are easily formed by volatilization at high temperature calcination. The valence band formation by Bi 6s orbitals is confirmed by the band structure and density of states obtained by DFT calculation as shown in Fig. 26. The conduction band is composed of V 3d as in other d^0 oxide photocatalysts. Although $BiVO_4$ does not show activity for H_2 evolution due to the low conduction level, it is noteworthy that the valence band formed with Bi 6s orbitals possesses the potential for water oxidation to form O_2 accompanied by 4-electron oxidation. $BiVO_4$ is also used for the decomposition of endocrine disruptors such as nonylphenol[252] and degradation of Methylene Blue,[253,254] Methyl Orange,[255–258] Rhodamine B,[259,260] 4-*n*-alkylphenol,[261,262] 4-*n*-nonylphenol,[261,262] aromatic hydrocarbons,[263] and benzopyrene.[264] OH radicals that are often an active species for photocatalytic oxidation of organic compounds are not involved with the degradation in the case of the $BiVO_4$ photocatalyst.[265]

$SnNb_2O_6$ shows activity for H_2 or O_2 evolution when suitable co-catalysts are loaded. Especially, $IrO_2/SnNb_2O_6$ shows relatively high activity for O_2 evolution.[229] Although $SnNb_2O_6$ is active for half reactions of water splitting under visible light irradiation overall water splitting is as yet not successful. Sn 5s orbitals in Sn^{2+} form a valence band as seen in $SnNb_2O_6$ while Sn 5s5p orbitals in Sn^{4+} form a conduction band as observed for Sr_2SnO_4 (Table 2).

$AgNbO_3$ with a perovskite structure and Ag_3VO_4 are active for O_2 evolution. $AgLi_{1/3}Ti_{2/3}O_2$ and $AgLi_{1/3}Sn_{2/3}O_2$ with delafossite structure are synthesized by treating layered compounds Li_2TiO_3 and Li_2SnO_3 with molten $AgNO_3$ through ion exchange of Li^+ for Ag^+ and show activities for O_2 evolution from an aqueous silver nitrate solution under visible light irradiation. The visible light responses of $AgNbO_3$, $AgLi_{1/3}Ti_{2/3}O_2$ and $AgLi_{1/3}Sn_{2/3}O_2$ are due to the band gap excitation between conduction bands consisting of either Nb 4d or Ti 3d or Sn 5s5p orbitals and valence bands consisting of Ag 4d orbitals.[125,231] $AgNbO_3$ is also active for the decomposition of endocrine disruptors such as nonylphenol.[266] Moreover, band engineering using the Ag 4d orbital is applied to develop solid solution photocatalysts of $AgNbO_3$–$SrTiO_3$ for degradations of 2-propanol[267,268] and CH_3CHO.[269]

7.1.5 Oxide photocatalysts with visible light response by sensitization[270–279]. Photocatalytic reactions under visible light irradiation by sensitization of wide band gap semiconductor photocatalysts have been studied as shown in Table 5. TiO_2 and $K_4Nb_6O_{17}$ loaded with various metal complexes and dyes respond to visible light for H_2 evolution according to a scheme as shown in Fig. 27. After an electron is excited from the HOMO to LUMO of a dye by visible light the electron is injected to a conduction band. H_2 evolves on the wide band gap photocatalyst. This sensitization is applied to a $Ru(bpy)_3^{2+}/K_4Nb_6O_{17}$ thin film electrode that gives a photocurrent responding to visible light.[280] Layered metal oxide photocatalysts intercalated with CdS are also active for H_2 evolution in the presence of sacrificial reagents. The layered metal oxides serve as H_2 evolution sites.

7.2 (Oxy)nitride and oxysulfide photocatalysts[281–296]

Domen and co-workers have reported (oxy)nitrides and oxysulfides as new types of visible light-driven photocatalysts as shown in Table 6. The valence bands of these photocatalysts consist of N 2p and S 3p orbitals, in addition to O 2p, resulting in the formation of narrow band gaps. These materials can utilize up to 500–600 nm visible light.

Oxynitride photocatalysts consisting of metal cations of Ti^{4+}, Nb^{5+} and Ta^{5+} with d^0 configuration are active for H_2 or O_2 evolution in the presence of sacrificial reagents. TaON and Ta_3N_5 give high quantum yields for O_2 evolution.

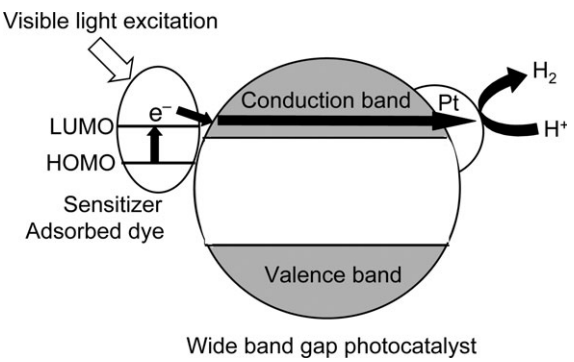

Fig. 27 Scheme of sensitized-type photocatalyst.

Table 6 (Oxy)nitride and oxysulfide photocatalysts for H_2 or O_2 evolution from aqueous solutions in the presence of sacrificial reagents under visible light irradiation[a]

		H_2 evolution[b]			O_2 evolution[c]			
Photocatalyst	BG/eV	Co-catal.	Activity/ μmol h^{-1}	QY (%)	Co-catal.	Activity/ μmol h^{-1}	QY (%)	Ref. (Year)
$LaTiO_2N$	2.1	Pt	30	0.15	IrO_2	41	1.5	281 (2002)
$Ca_{0.25}La_{0.75}TiO_{2.25}N_{0.75}$	2.0	Pt	5.5		IrO_2	230	5	281 (2002)
TaON	2.5	Ru	120	0.2		380	34	282–286 (2002)
Ta_3N_5	2.1	Pt	10	0.1 (420–600 nm)		420	10 (420–600 nm)	284, 286–288 (2002)
$CaNbO_2N$	1.9	Pt	1.5	—		46	—	289 (2002)
$CaTaO_2N$	2.5	Pt	15	—		0	—	290 (2004)
$SrTaO_2N$	2.1	Pt	20	—		0	—	290 (2004)
$BaTaO_2N$	2.0	Pt	15	—		0	—	290 (2004)
$LaTaO_2N$	2.0	Pt	20	—		0	—	289 (2002)
$Y_2Ta_2O_5N_2$	2.2	Pt-Ru	250	—		140	—	291 (2004)
$TiN_xO_yF_z$	2.2	—	—	—		30	—	292, 293 (2003)
$Sm_2Ti_2O_5S_2$	2.0	Pt	22	0.3		30	0.6	53, 294, 295 (2002)
La–In oxisulfide	2.6	Pt	10	0.2	IrO_2	7	0.1	296 (2007)

[a] Light source: 300 W Xe lamp with a cut-off filter (L42). [b] Sacrificial reagent: CH_3OH aq. [c] Sacrificial reagent: $AgNO_3$ aq. La_2O_3 or $La(NO)_3$ was added as a buffer for pH.

However, they are not active for water splitting into H_2 and O_2 without sacrificial reagents at the present stage. These materials can also be applied to photoelectrochemical cells.[297–299] Although metal sulfides such as CdS cannot evolve O_2 because of photocorrosion, $Sm_2Ti_2O_5S_2$, an oxysulfide with layered perovskite structure is active for the O_2 evolution.

8. Photocatalyst systems for water splitting under visible light irradiation

There are two types of photocatalyst systems for water splitting under visible light irradiation as shown in Fig. 28. Band engineering is indispensable to develop the single photocatalyst system as shown in Fig. 22. Some oxynitride photocatalysts are active for water splitting as mentioned in the next section. Two-photon systems, as seen in photosynthesis by green plants (*Z*-scheme), is another way to achieve overall water splitting as mentioned in section 8.3. The *Z*-scheme is composed of an H_2-evolution photocatalyst, an O_2-evolution photocatalyst, and an electron mediator. Photocatalysts that are active only for half reactions of water splitting as shown in Fig. 9 can be employed for the construction of the *Z* scheme: that is the merit of the *Z* scheme. Some photocatalysts listed in Table 4 are actually used for *Z*-scheme systems.

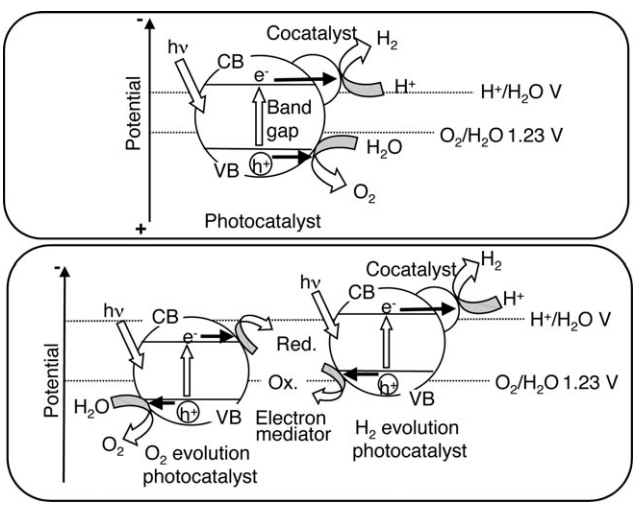

Fig. 28 Single- and two-photon photocatalyst systems for water splitting.

8.1 d^{10} metal nitrides[300–312]

Nitrides consisting of d^{10} metal cations are active for water splitting as shown in Table 7, in contrast to d^0 metal (oxy)nitrides. Ge_3N_4 shows activity under UV irradiation. This is the first example of a non-oxide powdered photocatalyst for water splitting.[300] GaN is the well known semiconductor that is used for a blue light emitting diode.[313] Native GaN powder is not active whereas GaN loaded with $Rh_{2-x}Cr_xO_3$ co-catalyst and Mg-doped GaN powders are active under UV irradiation. In contrast, GaN:ZnO solid solutions are active under visible light irradiation. The solid solutions are prepared by NH_3-treatment of a mixture of Ga_2O_3 and ZnO at 1123–1223 K for 5–30 h. Although native GaN and ZnO possess only UV absorption bands, the solid solutions have visible light absorption bands depending on the composition as shown in Fig. 29.[307] The visible light absorption is due to a Zn-related acceptor level and/or p–d repulsion between Zn 3d and N 2p + O 2p in addition to the contribution of N 2p to valence band formation.[312,314,315] Optimized GaN:ZnO with $Rh_{2-x}Cr_xO_3$ co-catalyst gives 5.9% of quantum yield.[311] Ge_3N_4:ZnO is also active under visible light irradiation.

8.2 d^0 metal oxides

$InTaO_4$[316,317] and $YBiWO_6$[318] have been reported for water splitting as single photocatalyst systems under visible light irradiation.

Table 7 (Oxy)nitride photocatalysts for water splitting[a]

Photocatalyst	BG/eV	Co-catalyst	Incident light/nm	Reactant solution	Activity/μmol h^{-1} H_2	Activity/μmol h^{-1} O_2	QY (%)	Ref. (Year)
Ge_3N_4	3.6	RuO_2	>200[b]	Pure water	1400	700	9 (at 300 nm)	300–303 (2005)
GaN	3.4	$Rh_{2-x}Cr_xO_3$	>300[c]	H_2SO_4 (pH 4.5)	19	9.5	0.7 (300–340 nm)	304 (2007)
GaN:Mg	3.4	RuO_2	>300[c]	Pure water	730	290		305, 306 (2006)
$(Ga_{0.88}Zn_{0.12})(N_{0.88}O_{0.12})$	2.6	$Rh_{2-x}Cr_xO_3$	>400[d]	H_2SO_4 (pH 4.5)	800	400	5.9 (420–440 nm)	50, 307–311 (2005)
$Zn_{1.44}GeN_{2.08}O_{0.38}$	2.7	RuO_2	>400[d]	Pure water	14.2	7.4		312 (2007)

[a] Light source: 450 W high pressure mercury lamp, reaction cell: inner irradiation cell. [b] Made of quartz. [c] Made of Pyrex. [d] Made of Pyrex filled with aqueous $NaNO_2$ solution as a filter.

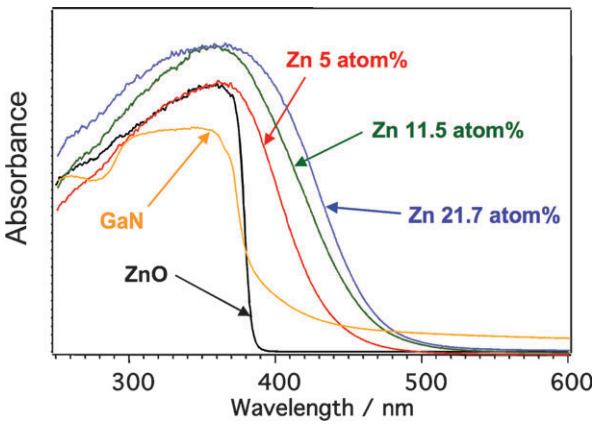

Fig. 29 Diffuse reflection spectra of $(Ga_{1-x}Zn_x)(N_{1-x}O_x)$ photocatalysts.[307]

8.3 *Z*-Scheme systems (two-photon process)[319–325]

Table 8 summarizes *Z*-scheme systems that work under visible light irradiation. Combined systems with Fe ion-WO_3,[326] Pt/TiO_2(anatase)–TiO_2(rutile)–IO_3^-/I^-[321,327] and Pt/TiO_2-(anatase)–Pt/WO_3–IO_3^-/I^-[321] are active for water splitting through a two-photon process under UV irradiation because an iron ion and TiO_2 respond to only UV. Combined systems with $Pt/SrTiO_3$:Cr/Ta for the H_2 evolution photocatalyst and Pt/WO_3 for the O_2 evolution photocatalyst can split water into H_2 and O_2 in stoichiometric amounts under visible light irradiation in the presence of an IO_3^-/I^- redox couple. Oxynitride photocatalysts, TaON, $CaTa_2O_2N$ and $BaTa_2O_2N$ can be used as H_2 evolution photocatalysts with a Pt/WO_3 of O_2 evolution photocatalyst. These photocatalyst systems respond to about 450-nm light, which is limited by the band gap of WO_3. The system of Pt/TaON with RuO_2/TaON is a unique combination and is active up to 500 nm. The *Z*-scheme system consisting of $Pt/SrTiO_3$:Rh and $BiVO_4$ or Bi_2MoO_6 is also active in the presence of an Fe^{3+}/Fe^{2+} redox couple. The system of $Pt/SrTiO_3$:Rh and $BiVO_4$ responds to 520-nm light, which corresponds to the energy and band gaps of $SrTiO_3$:Rh and $BiVO_4$ as shown in Fig. 30. Although the efficiency is low, solar hydrogen production from water has been accomplished using the *Z*-scheme system with powdered photocatalysts as shown in Fig. 31. It is a simple system: the sun is allowed to shine on the powders dispersed in aqueous solutions of iron ions and Co complexes which causes water splitting to form H_2 and O_2.

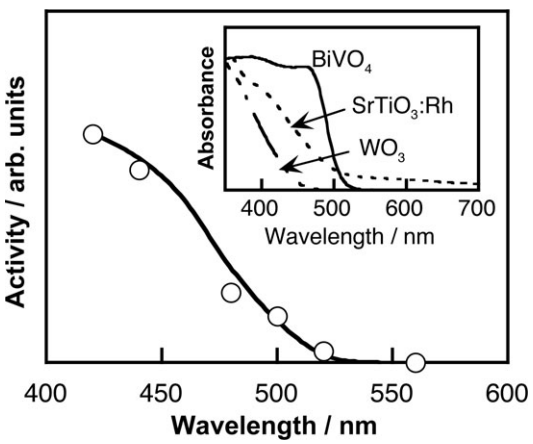

Fig. 30 Action spectrum for water splitting using (Ru/$SrTiO_3$:Rh)–(BVO_4)–$FeCl_3$.[325]

Table 8 *Z*-Scheme type photocatalysts for water splitting under visible light irradiation[a]

H_2 photocatalyst	O_2 photocatalyst	Mediator	Activity/μmol h^{-1} H_2	Activity/μmol h^{-1} O_2	QY (%)	Ref. (Year)
$Pt/SrTiO_3$:Cr,Ta	Pt/WO_3	IO^{3-}/I^-	16	8	1 (at 420 nm)	319–321 (2001)
Pt/TaON	RuO_2/TaON	IO^{3-}/I^-	3	1.5	0.1–0.2	322 (2008)
$Pt/CaTa_2O_2N$	Pt/WO_3	IO^{3-}/I^-	6.6	3.3	—	323 (2008)
$Pt/BaTa_2O_2N$	Pt/WO_3	IO^{3-}/I^-	4	2	—	323 (2008)
Pt/TaON	Pt/WO_3	IO^{3-}/I^-	24	12	0.4 (at 420 nm)	324 (2005)
$Pt/SrTiO_3$:Rh	$BiVO_4$	$Fe^{3+/2+}$	15	7.2	0.3 (at 440 nm)	325 (2004)
$Pt/SrTiO_3$:Rh	Bi_2MoO_6	$Fe^{3+/2+}$	19	8.9	0.2 (at 440 nm)	325 (2004)
$Pt/SrTiO_3$:Rh	WO_3	$Fe^{3+/2+}$	7.8	4.0	0.2 (at 440 nm)	325 (2004)

[a] Light source: 300 W Xe lamp with a cut-off filter (L42).

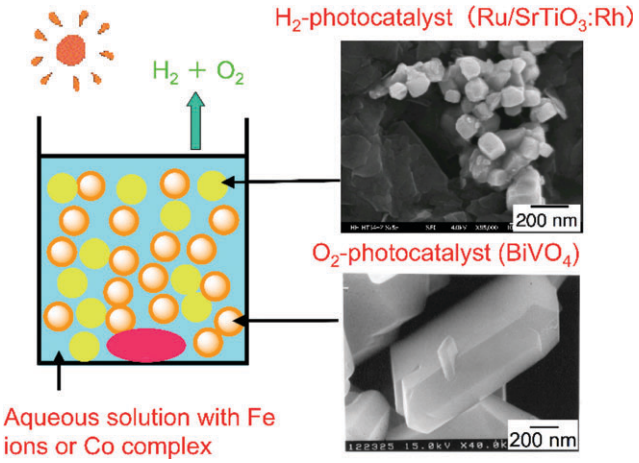

Fig. 31 Solar water splitting by *Z*-scheme photocatalyst system with nano-oxides.

9. Metal sulfide photocatalysts with visible light response for H_2 evolution from an aqueous solution containing a sacrificial reagent[328–349]

Metal sulfides are attractive materials as candidates of visible-light-driven photocatalysts. The valence band usually consists of S 3p orbitals the level of which is more negative than O 2p as shown in Fig. 22. Although instability is a drawback of metal sulfide photocatalysts the photocorrosion is suppressed by hole scavenger such as S^{2-} and SO_3^{2-}.

Many metal sulfide photocatalysts have been reported for H_2 evolution in the presence of sacrificial reagents as shown in Table 9.

9.1 Native visible-light driven photocatalysts[328–339]

CdS with a 2.4 eV-band gap is a well known metal sulfide photocatalyst that can produce H_2 under visible light irradiation in the presence of a sacrificial reagent.[328–331] CdS has been studied for a long time. ZnS with 3.6 eV-band gap is also a well-known photocatalyst for H_2 evolution though it responds to only UV. It shows high activity without any assistance of co-catalysts such as Pt. Therefore, ZnS is an attractive host photocatalyst for doping and preparing solid solutions as mentioned below. Photocatalytic H_2 evolution on $CuInS_2$, $CuIn_5S_8$, $AgGaS_2$ and $AgIn_5S_8$ has been reported in the presence of sacrificial reagents. These metal sulfides consist of elements of groups 11 and 13. $NaInS_2$ with layered structure and $ZnIn_2S_4$ with spinel structure are active. Feng and co-workers have reported unique photocatalysts of indium sulfide compounds with open-framework structure.[338,339]

9.2 Doped photocatalysts[330,340–342]

Fig. 32 shows diffuse reflection spectra of ZnS doped with various metal cations. Visible light absorption band tails are observed in addition to the band gap absorption band of the ZnS host. These spectra have typical shapes of doped photocatalysts being different from those of band gap transitions. These metal cation-doped ZnS photocatalysts show activities for H_2 evolution from aqueous solutions containing S^{2-} and/or SO_3^{2-} as electron donors. Loading of co-catalysts such as Pt is not necessary for the H_2 evolution, indicating that the high conduction band of the ZnS host is maintained after the doping of metal cations. Ag doping is also effective for a CdS photocatalyst.

9.3 Solid solution photocatalysts[330–332,343–348]

CdS and ZnS possess the same crystal structure indicating that they can form solid solutions. The CdS–ZnS solid solution is active for H_2 evolution.

Solid solutions of $AgInS_2$–ZnS, $CuInS_2$–ZnS and $CuInS_2$–$AgInS_2$–ZnS that are designed according to the strategy as shown in Fig. 23(c) show high photocatalytic activities for H_2 evolution from aqueous sulfide and sulfite solutions under

Table 9 Sulfide photocatalysts for H_2 evolution from aqueous solutions in the presence of sacrificial reagents

Photocatalyst	BG/ eV	Incident light/nm	Light source	Reactant solution	H_2 evolution/ μmol h^{-1}	QY (%)	Ref. (Year)
Pt/CdS	2.4	>390	500 W Hg	Na_2SO_3	40	35 (at 436 nm)	328–331 (1983)
ZnS	3.1	>200	200 W Hg	Na_2S + H_3PO_2 + NaOH	13 000	90 (at 313 nm)	332, 333 (1984)
$CuInS_2$		>300	400 W Xe	Na_2SO_3	0.3		334 (1992)
$CuIn_5S_8$		>300	400 W Xe	Na_2SO_3	1.8	0.02 (at 460 nm)	334 (1992)
Rh/$AgGaS_2$	2.6	>420	300 W Xe	Na_2S + K_2SO_3	1340	25 (at 440 nm)	17 (2006)
Pt/$AgIn_5S_8$	1.8	>420	400 W Xe	Na_2S + K_2SO_3	60	5.3 (at 411.2 nm)	335 (2007)
Pt/$NaInS_2$	2.3	>420	300 W Xe	K_2SO_3	470	6 (at 440 nm)	336 (2002)
Pt/$ZnIn_2S_4$	2.3	>420	300 W Xe	Na_2S + Na_2SO_3	77		337 (2003)
$Na_{10}In_{16}Cu_4S_{35}$	2.0	>420	300 W Xe	Na_2S	9	3.7 (at 420 nm)	338 (2005)
$In_{10}S_{18}^{6-}$: APE		>300	300 W Xe	Na_2SO_3	20		338 (2005)
$[Na_5(H_2O)_6]^{5+}[SIn_4(SIn_4)_{6/2}]^{5-}$	3.2	>300	300 W Xe	Na_2SO_3	2.4		339 (2005)
ZnS:Cu	2.5	>420	300 W Xe	K_2SO_3	450	3.7 (at 420 nm)	340 (1999)
ZnS:Ni	2.3	>420	300 W Xe	Na_2S + K_2SO_3	280		341 (2000)
ZnS:Pb, Cl	2.3	>420	300 W Xe	Na_2S + K_2SO_3	40		342 (2003)
Pt/CdS:Ag	2.35	>300	900 W Xe	Na_2S + Na_2SO_3	11 440	25 (at 450 nm)	329 (1986)
CdS–ZnS	2.35	>400	300 W Hg	Na_2S + Na_2SO_3	250	0.60	329–331 (2006)
Pt/$AgInZn_7S_9$	2.4	>420	300 W Xe	Na_2S + K_2SO_3	940	20 (at 420 nm)	343,344 (2004)
Pt/$Cu_{0.09}In_{0.09}Zn_{1.82}S_2$	2.35	>420	300 W Xe	Na_2S + K_2SO_3	1200	12.5 (at 420 nm)	345 (2005)
Ru/$Cu_{0.25}Ag_{0.25}In_{0.5}ZnS_2$	2.0	>420	300 W Xe	Na_2S + K_2SO_3	2300	7.4 (at 520 nm)	346,347
Pt/$AgGa_{0.9}In_{0.1}S_2$	2.4	>420	450 W Hg	Na_2S + Na_2SO_3	350		348 (2008)
Pt/$[In(OH)_yS_z]$:Zn	2.2	>420	300 W Xe	Na_2S + Na_2SO_3	67	0.59 (at 420 nm)	349 (2004)

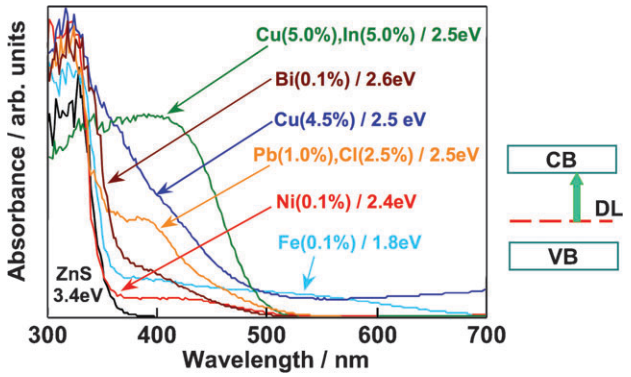

Fig. 32 Diffuse reflection spectra of metal ion-doped ZnS photocatalysts.

visible light irradiation. A solid solution photocatalyst of $AgGa_{0.9}In_{0.1}S_2$ is also active. The solid solution formation is usually confirmed by X-ray diffraction. Peaks of XRD shift with the composition of the solid solution according to the difference in ionic radii between metal cations. The diffuse reflectance spectra of $AgInS_2$–$CuInS_2$–ZnS solid solutions shift monotonically with the composition of the solid solution as shown in Fig. 33. DFT calculation indicates that the levels of the conduction band consisting of Zn 4s4p and In 5s5p, and of the valence band consisting of Cu 3d, Ag 4d and S 3p, shift with the varying composition. $Ru/Cu_{0.25}Ag_{0.25}In_{0.5}ZnS_2$ shows an excellent activity for H_2 evolution with a solar simulator (AM-1.5). These sulfide solid solution photocatalysts can utilize visible light of wavelengths up to about 700 nm. Moreover, solid solutions of $AgInS_2$-$CuInS_2$ are black photocatalysts with about 1.5 eV band gap for H_2 evolution. The black photocatalysts can utilize near-infrared radiation up to 820 nm. The authors have demonstrated solar hydrogen products from an aqueous Na_2S + K_2SO_3 solution using the $AgInS_2$–$CuInS_2$–ZnS solid solution photocatalyst and a reactor of 1 m^2. H_2 evolution at a rate of about 2 L/m^2 h was observed in November in Tokyo. This photocatalytic H_2 evolution will be important if abundant sulfur compounds in chemical industries or nature can be used as electron donors as

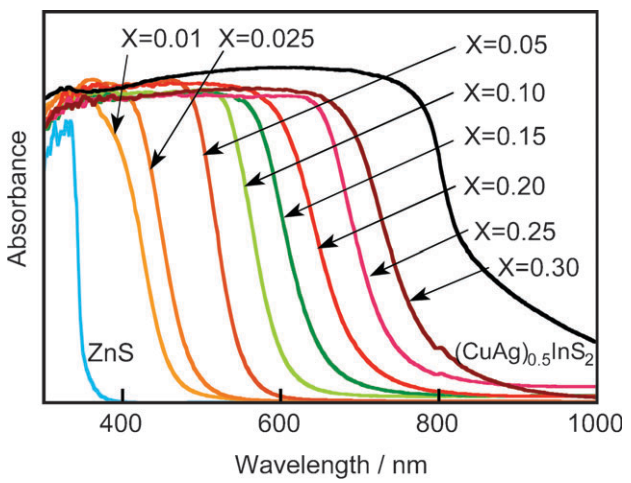

Fig. 33 Diffuse reflection spectra of $(CuAg)_xIn_{2x}Zn_{2(1-2x)}S_2$ solid solution.[346]

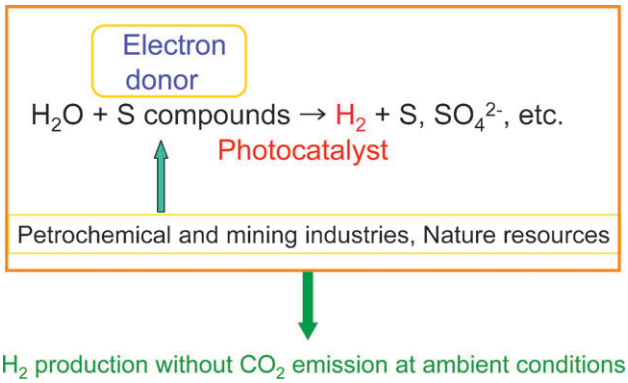

Fig. 34 Solar H_2 production using abundant sulfur compounds and metal sulfide photocatalysts.

shown in Fig. 34. Ideally, this reaction produces H_2 at ambient temperature and pressure but does not consume fossil fuels and does not emit CO_2. It should be noted that the photocatalytic H_2 evolution is not a solar energy conversion because the change in the Gibbs free energy is not so positive. Toji's group have studied CdS and ZnS photocatalysts with shell structure in the presence of an electron donor aiming at solar hydrogen production.[350]

$AgInS_2$–ZnS and $CuInS_2$–ZnS solid solution materials are applied to unique luminescent materials of which emission wavelengths are tuneable with the ratio of the solid solutions.[351–353]

10. Conclusions

Energy and environment issues are discussed in literature.[354–359] Solar water splitting including photocatalytic processes is focused on as a candidate of the science and technology for solving the issues in the future.[354,358,359] The number of photocatalysts for water splitting was very limited about twenty years ago. Furthermore, the only well-known visible light driven photocatalysts were CdS and WO_3 for H_2 and O_2 evolution, respectively, even in the presence of sacrificial reagents. Now, many photocatalyst materials have been developed as introduced in the present review paper. So, we are sure that this research area is progressing. For example, a highly efficient water splitting was achieved using a powdered photocatalyst of $NiO/NaTaO_3$:La under UV irradiation. The finding has proven that highly efficient water splitting is actually possible using powered photocatalysts. New powdered photocatalyst systems of oxynitrides such as $Cr_xRh_{2-x}O_3$/GaN:ZnO and *Z*-scheme systems such as Ru/$SrTiO_3$:Rh-$BiVO_4$ have been developed for overall water splitting under visible light irradiation after about 35 years from the report of the Honda–Fujishima effect. Solar water splitting is confirmed using the Ru/$SrTiO_3$:Rh–$BiVO_4$ photocatalyst system. Moreover, in the presence of sulfur compounds as electron donors, the sulfide solid solution photocatalysts $AgInS_2$–$CuInS_2$–ZnS are highly active for H_2 evolution under solar light irradiation. H_2 is thus realistically obtained under sunlight irradiation. Thus, the library of photocatalyst materials has become plentiful. The photocatalyst library will give information on factors affecting

photocatalytic abilities and the further development of new photocatalysts. The science for understanding photocatalytic processes is also developed.[40,168,251,360,361]

The target for efficiency for water splitting into H_2 and O_2 is 30% in terms of a quantum yield at 600 nm in this research field. This efficiency gives about 5% of solar energy conversion. The $Cr_xRh_{2-x}O_3$/GaN:ZnO and Ru/$SrTiO_3$:Rh-$BiVO_4$ photocatalysts respond to about 500 nm for overall water splitting so approaching this target but the quantum yield is still low. So, surveying photocatalyst materials are still important. It will be also important to construct the operating system for photocatalytic hydrogen production. Such an achievement will contribute to global energy and environmental issues in the future resulting in bringing about an energy revolution.

Acknowledgements

This work was supported by the Core Research for Evolutional Science and Technology (CREST) program of the Japan Science and Technology (JST) Agency, and a Grant-in-Aid for Priority Area Research from the Ministry of Education, Culture, Science, and Technology. The authors thank Dr Kato, Dr Tsuji, Prof. Domen, Prof. Kakihana, Prof. Kobayashi, Prof. Kohtani, Prof. Onishi and Prof. Torimoto for their collaborations and valuable discussions.

References

1 A. Fujishima, T. N. Rao and D. A. Tryk, *J. Photochem. Photobiol., C*, 2000, **1**, 1.
2 A. Fujishima, X. Zhang and D. A. Tryk, *Int. J. Hydrogen Energy*, 2007, **32**, 2664.
3 A. Fujishima and K. Honda, *Nature*, 1972, **238**, 37.
4 M. Grätzel, *Energy Resources through Photochemistry and Catalysis*, Academic Press, New York, 1983.
5 N. Serpone and E. Pelizzetti, *Photocatalysis*, Wiley, New York, 1989.
6 H. Yoneyama, *Crit. Rev. Solid State Mater. Sci.*, 1993, **18**, 69.
7 A. Kudo, *Hyomen*, 1998, **36**, 625 [in Japanese].
8 K. Domen, J. N. Kondo, M. Hara and T. Takata, *Bull. Chem. Soc. Jpn.*, 2000, **73**, 1307.
9 H. Arakawa and K. Sayama, *Catal. Surv. Jpn.*, 2000, **4**, 75.
10 K. Domen, M. Hara, J. N. Kondo, T. Takata, A. Kudo, H. Kobayashi and Y. Inoue, *Korean J. Chem. Eng.*, 2001, **18**, 862.
11 A. Kudo, *J. Ceram. Soc. Jpn.*, 2001, **109**, 81.
12 A. Kudo, *Catal. Surv. Asia*, 2003, **7**, 31.
13 Z. Zou and H. Arakawa, *J. Photochem. Photobiol., A*, 2003, **158**, 145.
14 H. Yamashita, M. Takeuchi and M. Anpo, *Encyclopedia of Nanoscience and Nanotechnology*, American Scientific Publishers, California, 2004, **10**, p. 639.
15 M. Anpo, S. Dohshi, M. Kitano, Y. Hu, M. Takeuchi and M. Matsuoka, *Annu. Rev. Mater. Res.*, 2005, **35**, 1.
16 J. S. Lee, *Catal. Surv. Asia*, 2005, **9**, 217.
17 A. Kudo, *Int. J. Hydrogen Energy*, 2006, **31**, 197.
18 Y. Inoue, *Chem. Ind.*, 2006, **108**, 623.
19 W. Zhang, S. B. Park and E. Kim, *Photo/Electrochemistry and Photobiology in the Environment, Energy and Fuel*, 2006, 295.
20 K. Maeda, K. Teramura, N. Saito, Y. Inoue, H. Kobayashi and K. Domen, *Pure Appl. Chem.*, 2006, **78**, 2267.
21 W. Shanguan, *Sci. Technol. Adv. Mater.*, 2007, **8**, 76.
22 A. Kudo, *Pure Appl. Chem.*, 2007, **79**, 1917.
23 A. Kudo, *Int. J. Hydrogen Energy*, 2007, **32**, 2673.
24 K. Maeda and K. Domen, *J. Phys. Chem. C*, 2007, **111**, 7851.
25 K. Maeda, K. Teramura and K. Domen, *Catal. Surv. Asia*, 2007, **11**, 145.
26 S. Ekambaram, *J. Alloys Compd.*, 2008, **448**, 238.
27 M. Laniecki, *Ceram. Eng. Sci. Proc.*, 2008, **28**, 23.
28 F. E. Osterloh, *Chem. Mater.*, 2008, **20**, 35.
29 J. Nozik, *Annu. Rev. Phys. Chem.*, 1978, **29**, 189.
30 Y. V. Pleskov and Y. Y. Gurevich, in *Semiconductor Photoelectrochemistry*, ed. P. N. Bartlett, Plenum, New York, 1986.
31 K. Tomita, V. Petrykin, M. Kobayashi, M. Shiro, M. Yoshimura and M. Kakihana, *Angew. Chem., Int. Ed.*, 2006, **45**, 2378.
32 Y. Oosawa and M. Gätzel, *J. Chem. Soc., Faraday Trans. 1*, 1988, **84**, 197.
33 T. Kawai and T. Sakata, *Nature (London, U. K.)*, 1979, **282**, 283.
34 T. Kawai and T. Sakata, *J. Chem. Soc., Chem. Commun.*, 1979, 1047.
35 T. Kawai and T. Sakata, *Nature (London, U. K.)*, 1980, **286**, 474.
36 T. Kawai and T. Sakata, *J. Chem. Soc., Chem. Commun.*, 1980, 694.
37 T. Kawai and T. Sakata, *Chem. Lett.*, 1981, **10**, 81.
38 T. Sakata and T. Kawai, *Nouv. J. Chim.*, 1981, **5**, 579.
39 S. Ikeda, T. Takata, M. Komoda, M. Hara, J. N. Kondo, K. Domen, A. Tanaka, H. Hosono and H. Kawazoe, *Phys. Chem. Chem. Phys.*, 1999, **1**, 4485.
40 B. Ohtani, *Chem. Lett.*, 2008, **37**, 217.
41 S. Sato and J. M. White, *Chem. Phys. Lett.*, 1980, **72**, 83.
42 J.-M. Lehn, J.-P. Sauvage and R. Ziessel, *Nouv. J. Chim.*, 1980, **4**, 623.
43 K. Yamaguti and S. Sato, *J. Chem. Soc., Faraday Trans. 1*, 1985, **81**, 1237.
44 G. R. Bamwenda, S. Tshbota, T. Nakamura and M. Haruta, *J. Photochem. Photobiol., A*, 1995, **89**, 177.
45 A. Iwase, H. Kato and A. Kudo, *Catal. Lett.*, 2006, **108**, 7.
46 K. Domen, S. Naito, S. Soma, M. Onishi and K. Tamaru, *J. Chem. Soc., Chem. Commun.*, 1980, 543.
47 T. Kawai and T. Sakata, *Chem. Phys. Lett.*, 1980, **72**, 87.
48 Y. Inoue, O. Hayashi and K. Sato, *J. Chem. Soc., Faraday Trans.*, 1990, **86**, 2277.
49 K. Maeda, K. Teramura, D. Lu, N. Saito, Y. Inoue and K. Domen, *Angew. Chem., Int. Ed.*, 2006, **45**, 7806.
50 K. Maeda, K. Teramura, D. Lu, N. Saito, Y. Inoue and K. Domen, *J. Catal.*, 2006, **243**, 303.
51 A. Iwase, H. Kato and A. Kudo, *Chem. Lett.*, 2005, **34**, 946.
52 M. Hara, C. C. Waraksa, J. T. Lean, B. A. Lewis and T. E. Mallouk, *J. Phys. Chem. A*, 2000, **104**, 5275.
53 A. Ishikawa, T. Takata, J. N. Kondo, M. Hara, H. Kobayashi and K. Domen, *J. Am. Chem. Soc.*, 2002, **124**, 13547.
54 A. Kudo, K. Domen, K. Maruya and T. Onishi, *Chem. Phys. Lett.*, 1987, **133**, 517.
55 K. Sayama and H. Arakawa, *J. Chem. Soc., Faraday Trans.*, 1997, **93**, 1647.
56 S. Tabata, N. Nishida, Y. Masaki and K. Tabata, *Catal. Lett.*, 1995, **34**, 245.
57 S.-C. Moon, H. Mametsuka, E. Suzuki and M. Anpo, *Chem. Lett.*, 1998, **27**, 117.
58 H. Mizoguchi, K. Ueda, M. Orita, S. C. Moon, K. Kajihara, M. Hirano and H. Hosono, *Mater. Res. Bull.*, 2002, **37**, 2401.
59 K. Domen, S. Naito, T. Onishi, T. Tamaru and M. Soma, *J. Phys. Chem.*, 1982, **86**, 3657.
60 K. Domen, S. Naito, T. Onishi and K. Tamaru, *Chem. Phys. Lett.*, 1982, **92**, 433.
61 K. Domen, A. Kudo, T. Onishi, N. Kosugi and H. Kuroda, *J. Phys. Chem.*, 1986, **90**, 292.
62 K. Domen, A. Kudo and T. Ohnishi, *J. Catal.*, 1986, **102**, 92.
63 A. Kudo, A. Tanaka, K. Domen and T. Onishi, *J. Catal.*, 1988, **111**, 296.
64 K. Yamaguti and S. Sato, *Nouv. J. Chim.*, 1986, **10**, 217.
65 H. Jeong, T. Kim, D. Kim and K. Kim, *Int. J. Hydrogen Energy*, 2006, **31**, 1142.
66 Y. G. Ko and W. Y. Lee, *Catal. Lett.*, 2002, **83**, 157.
67 T. Takata, Y. Furumi, K. Shinohara, A. Tanaka, M. Hara, J. N. Kondo and K. Domen, *Chem. Mater.*, 1997, **9**, 1063.
68 S. Ikeda, M. Hara, J. N. Kondo, K. Domen, H. Takahashi, T. Okubo and M. Kakihana, *Chem. Mater.*, 1998, **10**, 72.
69 J. Kim, D. W. Hwang, H. G. Kim, S. W. Bae, J. S. Lee, W. Li and S. H. Oh, *Top. Catal.*, 2005, **35**, 295.
70 H. G. Kim, D. W. Hwang, J. Kim, Y. G. Kim and J. S. Lee, *Chem. Commun.*, 1999, 1077.
71 A. Kim, D. W. Hwang, S. W. Bae, Y. G. Kim and J. S. Lee, *Korean J. Chem. Eng.*, 2001, **18**, 941.

72 J. Kim, D. W. Hwang, H. G. Kim, S. W. Bae, S. M. Ji and J. S. Lee, *Chem. Commun*., 2002, 2488.
73 D. W. Hwang, J. S. Lee, W. Li and S. H. Oh, *J. Phys. Chem. B*, 2003, **107**, 4963.
74 H. G. Kim, D. W. Hwang, S. W. Bae, J. H. Jung and J. S. Lee, *Catal. Lett*., 2003, **91**, 193.
75 H. G. Kim, S. M. Ji, J. S. Jang, S. W. Bae and J. S. Lee, *Korean J. Chem. Eng*., 2004, **21**, 970.
76 R. Abe, M. Higashi, K. Sayama, Y. Abe and H. Sugihara, *J. Phys. Chem. B*, 2006, **110**, 2219.
77 H. Song, P. Cai, Y. Huabing and C. Yan, *Catal. Lett*., 2007, **113**, 54.
78 S. M. Ji, H. Jun, J. S. Jang, H. C. Son, P. H. Borse and J. S. Lee, *J. Photochem. Photobiol., A*, 2007, **189**, 141.
79 V. R. Reddy, D. W. Hwang and J. S. Lee, *Catal. Lett*., 2003, **90**, 39.
80 H. Takahashi, M. Kakihana, Y. Yamashita, K. Yoshida, S. Ikeda, M. Hara and K. Domen, *J. Alloys Compd*., 1999, **285**, 77.
81 Y. Inoue, T. Kubokawa and K. Sato, *J. Chem. Soc., Chem. Commun*., 1990, 1298.
82 Y. Inoue, T. Kubokawa and K. Sato, *J. Phys. Chem*., 1991, **95**, 4059.
83 Y. Inoue, S. Ogura, M. Kohno and K. Sato, *Appl. Surf. Sci*., 1997, **121/122**, 521.
84 S. Ogura, K. Sato and Y. Inoue, *Phys. Chem. Chem. Phys*., 2000, **2**, 2449.
85 Y. Inoue, T. Niiyama, Y. Asai and K. Sato, *J. Chem. Soc., Chem. Commun*., 1992, 579.
86 Y. Inoue, Y. Asai and K. Sato, *J. Chem. Soc., Faraday Trans*., 1994, **90**, 797.
87 Y. Inoue, M. Kohno, S. Ogura and K. Sato, *Chem. Phys. Lett*., 1997, **267**, 72.
88 Y. Inoue, M. Kohno, S. Ogura and K. Sato, *J. Chem. Soc., Faraday Trans*., 1997, **93**, 2433.
89 Y. Inoue, M. Kohno, T. Kaneko, S. Ogura and K. Sato, *J. Chem. Soc., Faraday Trans*., 1998, **94**, 89.
90 T. Sato, M. Kakihana, M. Arima, K. Yoshida, Y. Yamashita, M. Yashima and M. Yoshimura, *Appl. Phys. Lett*., 1996, **69**, 2053.
91 R. Abe, M. Higashi, Z. G. Zou, K. Sayama and Y. Abe, *Chem. Lett*., 2004, **33**, 954.
92 M. Higashi, R. Abe, K. Sayama, H. Sugihara and Y. Abe, *Chem. Lett*., 2005, **34**, 1122.
93 K. Sayama and H. Arakawa, *J. Phys. Chem*., 1993, **97**, 531.
94 K. Sayama and H. Arakawa, *J. Photochem. Photobiol., A*, 1994, **77**, 243.
95 K. Sayama and H. Arakawa, *J. Photochem. Photobiol., A*, 1996, **94**, 67.
96 V. R. Reddy, D. W. Hwang and J. S. Lee, *Korean J. Chem. Eng*., 2003, **20**, 1026.
97 J. J. Zou, C. J. Liu and Y. P. Zhang, *Langmuir*, 2006, **22**, 2334.
98 K. Domen, A. Kudo, A. Shinozaki, A. Tanaka, K. Maruya and T. Onishi, *J. Chem. Soc., Chem. Commun*., 1986, 356.
99 K. Domen, A. Kudo, M. Shibata, A. Tanaka, K. Maruya and T. Onishi, *J. Chem. Soc., Chem. Commun*., 1986, 1706.
100 A. Kudo, A. Tanaka, K. Domen, K. Maruya, K. Aika and T. Onishi, *J. Catal*., 1988, **111**, 67.
101 A. Kudo, K. Sayama, A. Tanaka, K. Asakura, K. Domen, K. Maruya and T. Onishi, *J. Catal*., 1989, **120**, 337.
102 K. Domen, A. Kudo, A. Tanaka and T. Onishi, *Catal. Today*, 1990, **8**, 77.
103 K. Sayama, A. Tanaka, K. Domen, K. Maruya and T. Onishi, *J. Phys. Chem*., 1991, **95**, 1345.
104 K. Sayama, A. Tanaka, K. Domen, K. Maruya and T. Onishi, *Catal. Lett*., 1990, **4**, 217.
105 K. Sayama, H. Arakawa and K. Domen, *Catal. Today*, 1996, **28**, 175.
106 S. Ikeda, A. Tanaka, K. Shinohara, M. Hara, J. N. Kondo, K. Maruya and K. Domen, *Microporous Mesoporous Mater*., 1997, **9**, 253.
107 K. H. Chung and D. C. Park, *J. Photochem. Photobiol., A*, 1998, **129**, 53.
108 K. Sayama, K. Yase, H. Arakawa, K. Asakura, A. Tanaka, K. Domen and T. Onishi, *J. Photochem. Photobiol., A*, 1998, **114**, 125.
109 A. Kudo, H. Kato and S. Nakagawa, *J. Phys. Chem. B*, 2000, **104**, 571.
110 H. Kato and A. Kudo, *J. Photochem. Photobiol., A*, 2001, **145**, 129.
111 M. Yoshino, M. Kakihana, W. S. Cho, H. Kato and A. Kudo, *Chem. Mater*., 2002, **14**, 3369.
112 Y. Miseki, H. Kato and A. Kudo, *Chem. Lett*., 2006, **35**, 1052.
113 Y. Ebina, N. Sakai and T. Sasaki, *J. Phys. Chem. B*, 2005, **109**, 17212.
114 A. Kudo, S. Nakagawa and H. Kato, *Chem. Lett*., 1999, **28**, 1197.
115 Y. Miseki, H. Kato and A. Kudo, *Chem. Lett*., 2005, **34**, 54.
116 R. Abe, M. Higashi, Z. G. Zou, K. Sayama and H. Arakawa, *J. Phys. Chem. B*, 2004, **108**, 811.
117 H. Kato and A. Kudo, *Chem. Phys. Lett*., 1998, **295**, 487.
118 Y. Takahara, J. N. Kondo, T. Takata, D. Lu and K. Domen, *Chem. Mater*., 2001, **13**, 1194.
119 A. Kudo, H. Okutomi and H. Kato, *Chem. Lett*., 2000, **29**, 1212.
120 A. Kudo and H. Kato, *Chem. Lett*., 1997, **26**, 867.
121 T. Kurihara, H. Okutomi, Y. Miseki, H. Kato and A. Kudo, *Chem. Lett*., 2006, **35**, 274.
122 H. Kato and A. Kudo, *J. Phys. Chem. B*, 2001, **105**, 4285.
123 H. Kato and A. Kudo, *Catal. Lett*., 1999, **58**, 153.
124 H. Kato and A. Kudo, *Catal. Today*, 2003, **78**, 561.
125 H. Kato, H. Kobayashi and A. Kudo, *J. Phys. Chem. B*, 2002, **106**, 12441.
126 C. Mitsui, H. Nishiguchi, K. Fukamachi, T. Ishihara and Y. Takita, *Chem. Lett*., 1999, **28**, 1327.
127 T. Ishihara, H. Nishiguchi, K. Fukamachi and Y. Takita, *J. Phys. Chem. B*, 1999, **103**, 1.
128 A. Kudo and H. Kato, *Chem. Phys. Lett*., 2000, **331**, 373.
129 H. Kato, K. Asakura and A. Kudo, *J. Am. Chem. Soc*., 2003, **125**, 3082.
130 A. Iwase, H. Kato, H. Okutomi and A. Kudo, *Chem. Lett*., 2004, **33**, 1260.
131 S. Ikeda, M. Fubuki, Y. K. Takahara and M. Matsumura, *Appl. Catal., A*, 2006, **300**, 186.
132 T. Ishihara, N. S. Baik, N. Ono, H. Nishiguchi and Y. Takita, *J. Photochem. Photobiol., A*, 2004, **167**, 149.
133 H. Kato and A. Kudo, *Chem. Lett*., 1999, **28**, 1207.
134 K. Yoshioka, V. Petrykin, M. Kakihana, H. Kato and A. Kudo, *J. Catal*., 2005, **232**, 102.
135 K. Shimizu, Y. Tsuji, T. Hatamachi, K. Toda, T. Kodama, M. Sato and Y. Kitayama, *Phys. Chem. Chem. Phys*., 2004, **6**, 1064.
136 M. Machida, J. Yabunaka and T. Kijima, *Chem. Commun*., 1999, 1939.
137 M. Machida, J. Yabunaka and T. Kijima, *Chem. Mater*., 2000, **12**, 812.
138 M. Machida, J. Yabunaka, T. Kijima, S. Matsushita and M. Arai, *Int. J. Inorg. Chem*., 2001, **3**, 545.
139 M. Machida, K. Miyazaki, S. Matsushita and M. Arai, *J. Mater. Chem*., 2003, **13**, 1433.
140 K. Shimizu, S. Itoh, T. Hatamachi, T. Kodama, M. Sato and K. Toda, *Chem. Mater*., 2005, **17**, 5161.
141 W. Yao and J. Ye, *Chem. Phys. Lett*., 2007, **435**, 96.
142 T. Mitsuyama, A. Tsutsui, T. Hara, K. Ikeue and M. Machida, *Bull. Chem. Soc. Jpn*., 2008, **81**, 401.
143 H. Otsuka, K. Kim, A. Kouzu, I. Takimoto, H. Fujimori, Y. Sakata, H. Imamura, T. Matsumoto and K. Toda, *Chem. Lett*., 2005, **34**, 822.
144 Y. Li, G. Chen, C. Zhou and Z. Li, *Catal. Lett*., 2008, **123**, 80.
145 J. N. Kondo, M. Uchida, K. Nakajima, L. Daling, M. Hara and K. Domen, *Chem. Mater*., 2004, **16**, 4304.
146 M. Machida, S. Murakami and T. Kijima, *J. Phys. Chem. B*, 2001, **105**, 3289.
147 N. Saito, H. Kadowaki, H. Kobayashi, K. Ikarashi, H. Nishiyama and Y. Inoue, *Chem. Lett*., 2004, **33**, 2004.
148 H. Kadowaki, N. Saito, H. Nishiyama, H. Kobayashi, Y. Shimodaira and Y. Inoue, *J. Phys. Chem. C*, 2007, **111**, 439.
149 S. Ikeda, T. Itani, K. Nango and M. Matsumura, *Catal. Lett*., 2004, **98**, 229.
150 H. Kadowaki, N. Saito, H. Nishiyama and Y. Inoue, *Chem. Lett*., 2007, **36**, 440.
151 Y. Yuan, J. Zheng, X. Zhang, Z. Li, T. Yu, J. Ye and Z. Zou, *Solid State Ionics*, 2008, **178**, 1711.

152 M. Kakihana and K. Domen, *MRS Bull.*, 2000, **25**, 27.
153 J. G. Mavroides, J. A. Kafalas and D. F. Kolesar, *Appl. Phys. Lett.*, 1976, **28**, 241.
154 A. B. Ellis, S. W. Kaiser and M. S. Wrighton, *J. Phys. Chem.*, 1976, **80**, 1325.
155 A. Kudo, K. Domen, K. Maruya and T. Onishi, *Chem. Lett.*, 1987, **16**, 1019.
156 A. Kudo, K. Domen, K. Maruya and T. Onishi, *J. Catal.*, 1992, **135**, 300.
157 H. Kato and A. Kudo, *Phys. Chem. Chem. Phys.*, 2002, **4**, 2833.
158 H. Hagiwara, N. Ono, T. Inoue, H. Matsumoto and T. Ishihara, *Angew. Chem., Int. Ed.*, 2006, **45**, 1420.
159 H. Yoshida, S. Kato, K. Hirao, J. Nishimoto and T. Hattori, *Chem. Lett.*, 2007, **36**, 430.
160 J. F. Luan, S. R. Zheng, X. P. Hao, G. Y. Luan, X. Wu and Z. Zou, *J. Braz. Chem. Soc.*, 2006, **17**, 1368.
161 J. F. Luan, X. P. Hao, S. R. Zheng, G. Y. Luan and X. S. Wu, *J. Mater. Sci.*, 2006, **41**, 8001.
162 N. Ishizawa, F. Marumo, T. Kawamura and M. Kimura, *Acta Crystallogr., Sect. B: Struct. Crystallogr. Cryst. Chem.*, 1975, **31**, 1912.
163 N. Ishizawa, F. Marumo, T. Kawamura and M. Kimura, *Acta Crystallogr., Sect. B: Struct. Crystallogr. Cryst. Chem.*, 1976, **32**, 2564.
164 D. E. Scaife, *Sol. Energy*, 1980, **25**, 41.
165 M. P. Dare-Edwards, J. P. Goodenough, A. Hamnett and N. D. Nicholson, *J. Chem. Soc., Faraday Trans. 2*, 1981, **77**, 643.
166 M. Wiegel, M. H. J. Emond, E. R. Stobbe and G. J. Blasse, *J. Phys. Chem. Solids*, 1994, **55**, 773.
167 Z. Zou, J. Ye and H. Arakawa, *Chem. Phys. Lett.*, 2000, **332**, 271.
168 A. Yamakata, T. Ishibashi, H. Kato, A. Kudo and H. Onishi, *J. Phys. Chem. B*, 2003, **51**, 14383.
169 J. Sato, H. Kobayashi, N. Saito, H. Nishiyama and Y. Inoue, *J. Photochem. Photobiol., A*, 2003, **158**, 139.
170 J. Sato, H. Kobayashi and Y. Inoue, *J. Phys. Chem. B*, 2003, **107**, 7970.
171 J. Sato, N. Saito, H. Nishiyama and Y. Inoue, *J. Phys. Chem. B*, 2001, **105**, 6061.
172 J. Sato, N. Saito, H. Nishiyama and Y. Inoue, *J. Phys. Chem. B*, 2003, **107**, 7965.
173 J. Sato, N. Saito, H. Nishiyama and Y. Inoue, *Chem. Lett.*, 2001, **30**, 868.
174 N. Arai, N. Saito, H. Nishiyama, Y. Shimodaira, H. Kobayashi, Y. Inoue and K. Sato, *J. Phys. Chem. C*, 2008, **112**, 5000.
175 J. Sato, N. Saito, H. Nishiyama and Y. Inoue, *J. Photochem. Photobiol., A*, 2002, **148**, 85.
176 K. Ikarashi, J. Sato, H. Kobayashi, N. Saito, H. Nishiyama and Y. Inoue, *J. Phys. Chem. B*, 2002, **106**, 9048.
177 J. Sato, H. Kobayashi, K. Ikarashi, N. Saito, H. Nishiyama and Y. Inoue, *J. Phys. Chem. B*, 2004, **108**, 4369.
178 K. Ikarashi, J. Sato, H. Kobayashi, N. Saito, H. Nishiyama, Y. Simodaira and Y. Inoue, *J. Phys. Chem. B*, 2005, **109**, 22995.
179 T. Yanagida, Y. Sakata and H. Imamura, *Chem. Lett.*, 2004, **33**, 726.
180 Y. Sakata, Y. Matsuda, T. Yanagida, K. Hirata, H. Imamura and K. Teramura, *Catal. Lett.*, 2008, **125**, 22.
181 J. Tang, Z. Zou, J. Yin and J. Ye, *Chem. Phys. Lett.*, 2003, **382**, 175.
182 J. Tang, Z. Zou and J. Ye, *Chem. Mater.*, 2004, **16**, 1644.
183 J. Tang, Z. Zou, M. Katagiri, T. Kako and J. Ye, *Catal. Today*, 2004, **93**, 885.
184 J. Tang, Z. Zou and J. Ye, *Res. Chem. Intermed.*, 2005, **31**, 513.
185 M. Shibata, A. Kudo, A. Tanaka, K. Domen, K. Maruya and T. Onishi, *Chem. Lett.*, 1987, **16**, 1017.
186 A. Kudo and T. Kondo, *J. Mater. Chem.*, 1997, **7**, 777.
187 T. Sekine, J. Yoshimura, A. Tanaka, K. Domen, K. Maruya and T. Onishi, *Bull. Chem. Soc. Jpn.*, 1990, **63**, 2107.
188 M. Machida, X. W. Ma, H. Taniguchi, J. Yabunaka and T. Kijima, *J. Mol. Catal. A: Chem.*, 2000, **155**, 131.
189 A. Kudo and H. Kato, *Chem. Lett.*, 1997, **26**, 421.
190 K. Domen, Y. Ebina, T. Sekine, A. Tanaka, J. Kondo and C. Hirose, *Catal. Today*, 1993, **16**, 479.
191 Y. Ebina, A. Tanaka, J. N. Kondo and K. Domen, *Chem. Mater.*, 1996, **8**, 2534.
192 Y. Ebina, T. Sasaki, M. Harada and M. Watanabe, *Chem. Mater.*, 2002, **14**, 4390.
193 A. Kudo and S. Hijii, *Chem. Lett.*, 1999, **28**, 1103.
194 A. Kudo, A. Steinberg, A. J. Bard, A. Campion, M. A. Fox, T. E. Mallouk, S. E. Webber and J. M. White, *Catal. Lett.*, 1990, **5**, 61.
195 H. Kato, N. Matsudo and A. Kudo, *Chem. Lett.*, 2004, **33**, 1216.
196 A. Kudo and I. Mikami, *J. Chem. Soc., Faraday Trans.*, 1998, **94**, 2929.
197 M. P. Kapoor, S. Inagaki and H. Yoshida, *J. Phys. Chem. B*, 2005, **109**, 9231.
198 T. Sasaki, *J. Ceram. Soc. Jpn.*, 2007, **115**, 9.
199 O. C. Compton, E. C. Carroll, J. Y. Kim, D. S. Larsen and F. E. Osterloh, *J. Phys. Chem. C*, 2007, **111**, 14589.
200 O. C. Compton, C. H. Mullet, S. Chiang and F. E. Osterloh, *J. Phys. Chem. C*, 2008, **112**, 6202.
201 T. Yamase, *Chem. Rev.*, 1998, **98**, 307.
202 A. A. Krasnovsky and G. P. Brin, *Dokl. Akad. Nauk SSSR*, 1962, **147**, 656.
203 J. R. Darwent and A. Mills, *J. Chem. Soc., Faraday Trans. 2*, 1982, **78**, 359.
204 W. Erbs, J. Desilvestro, E. Borgarello and M. Grätzel, *J. Phys. Chem.*, 1984, **88**, 4001.
205 Y. Shimodaira, H. Kato, H. Kobayashi and A. Kudo, *J. Phys. Chem. B*, 2006, **110**, 17790.
206 D. Wang, J. Tang, Z. Zou and J. Ye, *Chem. Mater.*, 2005, **17**, 5177.
207 W. Yao and J. Ye, *Chem. Phys. Lett.*, 2008, **450**, 370.
208 A. Kudo and I. Mikami, *Chem. Lett.*, 1998, **10**, 1027.
209 H. Kato and A. Kudo, *J. Phys. Chem. B*, 2002, **106**, 5029.
210 R. Niishiro, H. Kato and A. Kudo, *Phys. Chem. Chem. Phys.*, 2005, **7**, 2241.
211 T. Ishii, H. Kato and A. Kudo, *J. Photochem. Photobiol., A*, 2004, **163**, 181.
212 R. Konta, T. Ishii, H. Kato and A. Kudo, *J. Phys. Chem. B*, 2004, **108**, 8992.
213 S. Nishimoto, M. Matsuda and M. Miyake, *Chem. Lett.*, 2006, **35**, 308.
214 D. W. Hwang, H. G. Kim, J. S. Jang, S. W. Bae, S. M. Ji and J. S. Lee, *Catal. Today*, 2004, **93**, 845.
215 D. W. Hwang, H. G. Kim, J. S. Lee, J. Kim, W. Le and S. H. Oh, *J. Phys. Chem. B*, 2005, **109**, 2093.
216 R. Niishiro, R. Konta, H. Kato, W. J. Chun, K. Asakura and A. Kudo, *J. Phys. Chem. C*, 2007, **111**, 17420.
217 Y. Shimodaira, H. Kato, H. Kobayashi and A. Kudo, *Bull. Chem. Soc. Jpn.*, 2007, **80**, 885.
218 J. Yoshimura, Y. Ebina, J. Kondo, K. Domen and A. Tanaka, *J. Phys. Chem.*, 1993, **97**, 1970.
219 H. G. Kim, D. W. Hwang and J. S. Lee, *J. Am. Chem. Soc.*, 2004, **126**, 8912.
220 H. G. Kim, O. S. Becker, J. S. Jang, S. M. Ji, P. H. Borse and J. S. Lee, *J. Solid State Chem.*, 2006, **179**, 1214.
221 A. Kudo, K. Ueda and H. Kato, *Catal. Lett.*, 1998, **53**, 229.
222 A. Kudo, K. Omori and H. Kato, *J. Am. Chem. Soc.*, 1999, **121**, 11459.
223 S. Tokunaga, H. Kato and A. Kudo, *Chem. Mater.*, 2001, **13**, 4624.
224 J. Q. Yu and A. Kudo, *Adv. Funct. Mater.*, 2006, **16**, 2163.
225 H. Liu, R. Nakamura and Y. Nakato, *ChemPhysChem*, 2005, **6**, 2499.
226 H. Liu, R. Nakamura and Y. Nakato, *Electrochem. Solid-State Lett.*, 2006, **9**, G187.
227 Y. Hosogi, K. Tanabe, H. Kato, H. Kobayashi and A. Kudo, *Chem. Lett.*, 2004, **33**, 28.
228 Y. Hosogi, H. Kato and A. Kudo, *Chem. Lett.*, 2006, **35**, 578.
229 Y. Hosogi, Y. Shimodaira, H. Kato, H. Kobayashi and A. Kudo, *Chem. Mater.*, 2008, **20**, 1299.
230 R. Konta, H. Kato, H. Kobayashi and A. Kudo, *Phys. Chem. Chem. Phys.*, 2003, **5**, 3061.
231 Y. Hosogi, H. Kato and A. Kudo, *J. Mater. Chem.*, 2008, **18**, 647.
232 R. Abe, H. Takami, N. Murakami and B. Ohtani, *J. Am. Chem. Soc.*, 2008, **130**, 7780.
233 J. Yu, J. Xiong, B. Cheng, Y. Yu and J. Wang, *J. Solid State Chem.*, 2005, **178**, 1968.
234 J. Tang, Z. Zou and J. Ye, *Catal. Lett.*, 2004, **92**, 53.
235 F. Amano, K. Nogami, R. Abe and B. Otani, *Chem. Lett.*, 2007, **36**, 1314.

236 F. Amano, K. Nogami, R. Abe and B. Otani, *J. Phys. Chem. C*, 2008, **112**, 9320.
237 H. Fu, C. Pan, W. Yao and Y. Zhu, *J. Phys. Chem. B*, 2005, **109**, 22432.
238 C. Zhang and Y. Zhu, *Chem. Mater.*, 2005, **17**, 3537.
239 S. Zhang, C. Zhang, Y. Man and Y. Zhu, *J. Solid State Chem.*, 2006, **179**, 62.
240 S. Zhu, T. Xu, H. Fu, J. Zhao and Y. Zhu, *Environ. Sci. Technol.*, 2007, **41**, 6234.
241 J. Wu, F. Duan, Y. Zheng and Y. Xie, *J. Phys. Chem. C*, 2007, **111**, 12866.
242 J. Li, X. Zhang, Z. Ai, F. Jia, L. Zhang and J. Lin, *J. Phys. Chem. C*, 2007, **111**, 6832.
243 S. Zhang, J. Shen, H. Fu, W. Dong, Z. Zheng and L. Shi, *J. Solid State Chem.*, 2007, **180**, 1165.
244 H. Xie, D. Shen, X. Wang and G. Shen, *Mater. Chem. Phys.*, 2007, **103**, 334.
245 H. Fu, C. Pan, L. Zhang and Y. Zhu, *Mater. Res. Bull.*, 2007, **42**, 696.
246 L. Wu, J. Bi, Z. Li, X. Wang and X. Fu, *Catal. Today*, 2008, **131**, 15.
247 H. Fu, S. Zhang, T. Xu, Y. Zhu and J. Chen, *Environ. Sci. Technol.*, 2008, **42**, 2085.
248 L. Zhou, W. Wang and L. Zhang, *J. Mol. Catal. A: Chem.*, 2007, **268**, 195.
249 C. A. Martinez-de la, S. O. Alfaro, E. L. Cuellar and U. O. Mendez, *Catal. Today*, 2007, **129**, 194.
250 R. Asahi, T. Morikawa, T. Ohwaki, K. Aoki and Y. Taga, *Science*, 2001, **293**, 269.
251 T. Ikeda, T. Nomoto, K. Eda, Y. Mizutani, H. Kato, A. Kudo and H. Onishi, *J. Phys. Chem. C*, 2008, **112**, 1167.
252 S. Kohtani, A. Koshiko, A. Kudo, K. Tokumura, Y. Ishigaki, A. Toriba, K. Hayakawa and R. Nakagaki, *Appl. Catal., B*, 2003, **46**, 573.
253 X. Zhang, Z. Ai, F. Jia, L. Zhang, X. Fan and Z. Zou, *Mater. Chem. Phys.*, 2007, **103**, 162.
254 H. Xu, H. Li, C. Wu, J. Chu, Y. Yan, H. Shu and Z. Gu, *J. Hazard. Mater.*, 2008, **153**, 877.
255 L. Zhou, W. Wang, S. Liu, L. Zhang, H. Xu and W. Zhu, *J. Mol. Catal. A: Chem.*, 2006, **252**, 120.
256 L. Ge, *Mater. Chem. Phys.*, 2008, **107**, 465.
257 L. Ge, *Mater. Lett.*, 2008, **62**, 926.
258 L. Ge, *J. Inorg. Mater.*, 2008, **23**, 449.
259 L. Zhou, W. Wang, L. Zhang, H. Xu and W. Zhu, *J. Phys. Chem. C*, 2007, **111**, 13659.
260 Y. Zheng, J. Wu, F. Duan and Y. Xie, *Chem. Lett.*, 2007, **36**, 520.
261 S. Kohtani, S. Makino, A. Kudo, K. Tokumura, Y. Ishigaki, T. Matsunaga, O. Nikaido, K. Hayakawa and R. Nakagaki, *Chem. Lett.*, 2002, **7**, 660.
262 S. Kohtani, J. Hiro, N. Yamamoto, A. Kudo, K. Tokumura and R. Nakagaki, *Catal. Commun.*, 2005, **6**, 185.
263 S. Kohtani, M. Tomohiro, K. Tokumura and R. Nakagaki, *Appl. Catal., B*, 2005, **58**, 265.
264 S. Kohtani, Y. Inaoka, K. Hayakawa and R. Nakagaki, *J. Adv. Oxid. Technol.*, 2007, **10**, 381.
265 S. Kohtani, K. Yoshida, T. Maekawa, A. Iwase, A. Kudo, H. Miyabe and R. Nakagaki, *Phys. Chem. Chem. Phys.*, 2008, **10**, 2986.
266 S. Kohtani, N. Yamamoto, K. Kitajima, A. Kudo, H. Kato, K. Tokumura, K. Hayakawa and R. Nakagaki, *Photo/Electrochem. Photobiol. Environ. Energy Fuel*, 2004, 173.
267 H. Irie, Y. Maruyama and K. Hashimoto, *J. Phys. Chem. C*, 2007, **111**, 1847.
268 G. Li, T. Kako, D. Wang, Z. Zou and J. Ye, *J. Solid State Chem.*, 2007, **180**, 2845.
269 D. Wang, T. Kako and J. Ye, *J. Am. Chem. Soc.*, 2008, **130**, 2724.
270 T. Kajiwara, K. Hasimoto, T. Kawai and T. Sakata, *J. Phys. Chem.*, 1982, **86**, 4516.
271 K. Hashimoto, T. Kawai and T. Sakata, *Nouv. J. Chim.*, 1983, **7**, 249.
272 T. Shimidzu, T. Iyoda and Y. Koide, *J. Am. Chem. Soc.*, 1985, **107**, 35.
273 Y. I. Kim, S. J. Atherton, E. S. Brigham and T. E. Mallouk, *J. Phys. Chem.*, 1993, **97**, 11802.
274 E. A. Malinka, G. L. Kamalov, S. V. Vodzinskii, V. I. Melnik and Z. I. Zhilina, *J. Photochem. Photobiol., A*, 1995, **90**, 153.
275 R. Abe, K. Sayama and H. Arakawa, *Chem. Phys. Lett.*, 2003, **379**, 230.
276 R. Abe, K. Sayama and H. Arakawa, *J. Photochem. Photobiol., A*, 2004, **166**, 115.
277 J. Yoshimura, A. Kudo, A. Tanaka, K. Domen, K. Maruya and T. Onishi, *Chem. Phys. Lett.*, 1988, **147**, 401.
278 J. Yoshimura, A. Tanaka, J. N. Kondo and K. Domen, *Bull. Chem. Soc. Jpn.*, 1995, **68**, 2439.
279 S. Tawkaew, Y. Fujishiro, S. Yin and T. Sato, *Colloids Surf., A*, 2001, **179**, 139.
280 Z. Tong, S. Takagi, H. Tachibana, K. Takagi and H. Inoue, *J. Phys. Chem. B*, 2005, **109**, 21612.
281 A. Kasahara, K. Nukumizu, G. Hitoki, T. Takata, J. N. Kondo, M. Hara, H. Kobayashi and K. Domen, *J. Phys. Chem. A*, 2002, **106**, 6750.
282 G. Hitoki, T. Takata, J. N. Kondo, M. Hara, H. Kobayashi and K. Domen, *Chem. Commun.*, 2002, 1698.
283 M. Hara, J. Nunoshige, T. Takata, J. N. Kondo and K. Domen, *Chem. Commun.*, 2003, 3000.
284 M. Hara, G. Hitoki, T. Takata, J. N. Kondo, H. Kobayashi and K. Domen, *Catal. Today*, 2003, **78**, 555.
285 M. Hara, T. Takata, J. N. Kondo and K. Domen, *Catal. Today*, 2004, **90**, 313.
286 T. Takata, G. Hitoki, J. N. Kondo, M. Hara, H. Kobayashi and K. Domen, *Res. Chem. Intermed.*, 2007, **33**, 13.
287 G. Hitoki, A. Ishikawa, J. N. Kondo, M. Hara and K. Domen, *Chem. Lett.*, 2002, **31**, 736.
288 Y. Lee, K. Nukumizu, T. Watanabe, T. Takata, M. Hara, M. Yoshimura and K. Domen, *Chem. Lett.*, 2006, **35**, 352.
289 G. Hitoki, T. Takata, J. N. Kondo, M. Hara, H. Kobayashi and K. Domen, *Electrochemistry (Tokyo, Jpn.)*, 2002, **70**, 463.
290 D. Yamasita, T. Takata, M. Hara, J. N. Kondo and K. Domen, *Solid State Ionics*, 2004, **172**, 591.
291 M. Liu, W. You, Z. Lei, G. Zhou, J. Yang, G. Wu, G. Ma, G. Luan, T. Takata, M. Hara, K. Domen and C. Lee, *Chem. Commun.*, 2004, 2192.
292 K. Nukumizu, J. Nunoshige, T. Takata, J. N. Kondo, M. Hara, H. Kobayashi and K. Domen, *Chem. Lett.*, 2003, **32**, 196.
293 K. Maeda, Y. Shimodaira, B. Lee, K. Teramura, D. Lu, H. Kobayashi and K. Domen, *J. Phys. Chem. C*, 2007, **111**, 18264.
294 A. Ishikawa, Y. Yamada, T. Takata, J. N. Kondo, M. Hara. H. Kobayashi and K. Domen, *Chem. Mater.*, 2003, **15**, 4442.
295 A. Ishikawa, T. Takata, T. Matsumura, J. N. Kondo, M. Hara. H. Kobayashi and K. Domen, *J. Phys. Chem. B*, 2004, **108**, 2637.
296 K. Ogisu, A. Ishikawa, K. Teramura, K. Toda, M. Hara and K. Domen, *Chem. Lett.*, 2007, **36**, 854.
297 A. Ishikawa, T. Takata, J. N. Kondo, M. Hara and K. Domen, *J. Phys. Chem. B*, 2004, **108**, 11049.
298 R. Abe, T. Takata, H. Sugihara and K. Domen, *Chem. Lett.*, 2005, **34**, 1162.
299 R. Nakamura, T. Tanaka and Y. Nakato, *J. Phys. Chem. B*, 2005, **109**, 8920.
300 J. Sato, N. Saito, Y. Yamada, K. Maeda, T. Takata, J. N. Kondo, M. Hara, H. Kobayashi, K. Domen and Y. Inoue, *J. Am. Chem. Soc.*, 2005, **127**, 4150.
301 Y. Lee, T. Watanabe, T. Takata, M. Hara, M. Yoshimura and K. Domen, *J. Phys. Chem. B*, 2006, **110**, 17563.
302 K. Maeda, N. Saito, D. Lu, Y. Inoue and K. Domen, *J. Phys. Chem. C*, 2007, **111**, 4749.
303 K. Maeda, N. Saito, Y. Inoue and K. Domen, *Chem. Mater.*, 2007, **19**, 4092.
304 K. Maeda, K. Teramura, N. Saito, Y. Inoue and K. Domen, *Bull. Chem. Soc. Jpn.*, 2007, **80**, 1004.
305 N. Arai, N. Saito, H. Nishiyama, Y. Inoue, K. Domen and K. Sato, *Chem. Lett.*, 2006, **35**, 796.
306 N. Arai, N. Saito, H. Nishiyama, K. Domen, H. Kobayashi, K. Sato and Y. Inoue, *Catal. Today*, 2007, **129**, 407.
307 K. Maeda, T. Takata, M. Hara, N. Saito, Y. Inoue, H. Kobayashi and K. Domen, *J. Am. Chem. Soc.*, 2005, **127**, 8286.
308 K. Maeda, K. Teramura, T. Takata, M. Hara, N. Saito, Y. Inoue, H. Kobayashi and K. Domen, *J. Phys. Chem. B*, 2005, **109**, 20504.
309 K. Maeda, K. Teramura, D. Lu, T. Takata, N. Saito, Y. Inoue and K. Domen, *Nature*, 2006, **440**, 295.

310 X. Sun, K. Maeda, F. M. Le, K. Teramura and K. Domen, *Appl. Catal., A*, 2007, **327**, 114.
311 K. Maeda, K. Teramura and K. Domen, *J. Catal*., 2008, **254**, 198.
312 Y. Lee, H. Terashita, Y. Shimodaira, K. Teramura, M. Hara, H. Kobayashi, K. Domen and M. Yashima, *J. Phys. Chem. C*, 2007, **111**, 1042.
313 S. Nakamura, *Solid State Commun*., 1997, **102**, 237.
314 T. Hirai, K. Maeda, M. Yoshida, J. Kubota, S. Ikeda, M. Matsumura and K. Domen, *J. Phys. Chem. C*, 2007, **111**, 18853.
315 L. L. Jensen, J. T. Muckerman and M. D. Newton, *J. Phys. Chem. C*, 2008, **112**, 3439.
316 Z. Zou, J. Ye, K. Sayama and H. Arakawa, *Nature*, 2001, **414**, 625.
317 Z. Zou, J. Ye and H. Arakawa, *J. Phys. Chem. B*, 2002, **106**, 13098.
318 H. Liu, W. Shangguan and Y. Teraoka, *J. Phys. Chem. C*, 2008, **112**, 8521.
319 K. Sayama, K. Mukasa, R. Abe, Y. Abe and H. Arakawa, *Chem. Commun*., 2001, 24169.
320 K. Sayama, K. Mukasa, R. Abe, Y. Abe and H. Arakawa, *J. Photochem. Photobiol., A*, 2002, **148**, 71.
321 R. Abe, K. Sayama and H. Sugihara, *J. Phys. Chem. B*, 2005, **109**, 16052.
322 M. Higashi, R. Abe, A. Ishikawa, T. Takata, B. Ohtani and K. Domen, *Chem. Lett*., 2008, **37**, 138.
323 M. Higashi, R. Abe, K. Teramura, T. Takata, B. Ohtani and K. Domen, *Chem. Phys. Lett*., 2008, **452**, 120.
324 R. Abe, T. Takata, H. Sugihara and K. Domen, *Chem. Commun*., 2005, 3829.
325 H. Kato, M. Hori, R. Konta, Y. Shimodaira and A. Kudo, *Chem. Lett*., 2004, **33**, 1348.
326 K. Sayama, R. Yoshida, H. Kusama, K. Okabe, Y. Abe and H. Arakawa, *Chem. Phys. Lett*., 1997, **277**, 387.
327 R. Abe, K. Sayama, K. Domen and H. Arakawa, *Chem. Phys. Lett*., 2001, **344**, 339.
328 M. Matsumura, Y. Saho and H. Tsubomura, *J. Phys. Chem*., 1983, **87**, 3807.
329 J. F. Reber and M. Rusek, *J. Phys. Chem*., 1986, **90**, 824.
330 N. Kakuta, K. H. Park, M. F. Finlayson, A. Ueno, A. J. Bard, A. Campion, M. A. Fox, S. E. Webber and J. M. White, *J. Phys. Chem*., 1985, **89**, 732.
331 C. Xing, Y. Zhang, W. Yan and L. Guo, *Int. J. Hydrogen Energy*, 2006, **31**, 2018.
332 J. F. Reber and K. Meier, *J. Phys. Chem*., 1984, **88**, 5903.
333 W. Ming, G. Wanzhen, L. Wenzhao, Z. Xiangwet, W. Fudong and Z. Shiting, *Stud. Surf. Sci. Catal*., 1995, **92**, 257.
334 K. Kobayakawa, A. Teranishi, T. Tsurumaki, Y. Sato and A. Fujishima, *Electrochim. Acta*, 1992, **37**, 465.
335 D. Chen and J. Ye, *J. Phys. Chem. Solids*, 2007, **68**, 2317.
336 A. Kudo, A. Nagane, I. Tsuji and H. Kato, *Chem. Lett*., 2002, **31**, 882.
337 Z. Lei, W. You, M. Liu, G. Zhou, T. Takata, M. Hara, K. Domen and C. Li, *Chem. Commun*., 2003, 2142.
338 N. Zheng, X. Bu, H. Vu and P. Feng, *Angew. Chem., Int. Ed*., 2005, **44**, 5299.
339 N. Zheng, X. Bu and P. Feng, *J. Am. Chem. Soc*., 2005, **127**, 5286.
340 A. Kudo and M. Sekizawa, *Catal. Lett*., 1999, 241.
341 A. Kudo and M. Sekizawa, *Chem. Commun*., 2000, 1371.
342 I. Tsuji and A. Kudo, *J. Photochem. Photobiol., A*, 2003, **156**, 249.
343 I. Tsuji, H. Kato and A. Kudo, *Chem. Commun*., 2002, 1958.
344 I. Tsuji, H. Kato, H. Kobayashi and A. Kudo, *J. Am. Chem. Soc*., 2004, **41**, 13406.
345 I. Tsuji, H. Kato, H. Kobayashi and A. Kudo, *J. Phys. Chem. B*, 2005, **109**, 7323.
346 I. Tsuji, H. Kato and A. Kudo, *Angew. Chem., Int. Ed*., 2005, **44**, 3565.
347 I. Tsuji, H. Kato and A. Kudo, *Chem. Mater*., 2006, **18**, 1969.
348 J. S. Jang, P. H. Borse, J. S. Lee, S. H. Choi and H. G. Kim, *J. Chem. Phys*., 2008, **128**, 154717.
349 Z. Lei, G. Ma, M. Liu, W. You, H. Yan, G. Wu, T. Takata, M. Hara, K. Domen and C. Li, *J. Catal*., 2006, **237**, 322.
350 T. Arai, S. Senda, Y. Sato, H. Takahashi, K. Shinoda, B. Jeyadevan and K. Toji, *Chem. Mater*., 2008, **20**, 1997.
351 H. Nakamura, W. Kato, M. Uehara, K. Nose, T. Omata, S. O. Y. Matuo, M. Miyazaki and H. Maeda, *Chem. Mater*., 2006, **18**, 3330.
352 T. Torimoto, T. Adachi, K. Okazaki, M. Sakuraoka, T. Shibayama, B. Ohtani, A. Kudo and S. Kuwabata, *J. Am. Chem. Soc*., 2007, **129**, 12388.
353 T. Kameyama, K. Okazaki, Y. Ichikawa, A. Kudo, S. Kuwabata and T. Torimoto, *Chem. Lett*., 2008, **37**, 700.
354 N. S. Lewis, *Nature*, 2001, **414**, 589.
355 K. W. J. Barnham, M. Mazzer and B. Clive, *Nat. Mater*., 2006, **5**, 161.
356 Editorial, *Nat. Mater*., 2006, **5**, 159.
357 Q. Schiermeier, J. Tollefson, T. Scully, A. Witze and O. Morton, *Nature*, 2008, **454**, 823.
358 K. Sanderson, *Nature*, 2008, **452**, 400.
359 R. Schloegl, *Nat. Mater*., 2008, **7**, 772.
360 H. Uetsuka, C. Pang, A. Sasahara and H. Onishi, *Langmuir*, 2005, **21**, 11802.
361 M. A. Henderson, J. M. White, H. Uetsuda and H. Onishi, *J. Catal*., 2006, **238**, 153.

